Koiliaris Panayiotis

3D Printed Soft Fluidic Actuator for an Assistive Hand Exoskeleton Device

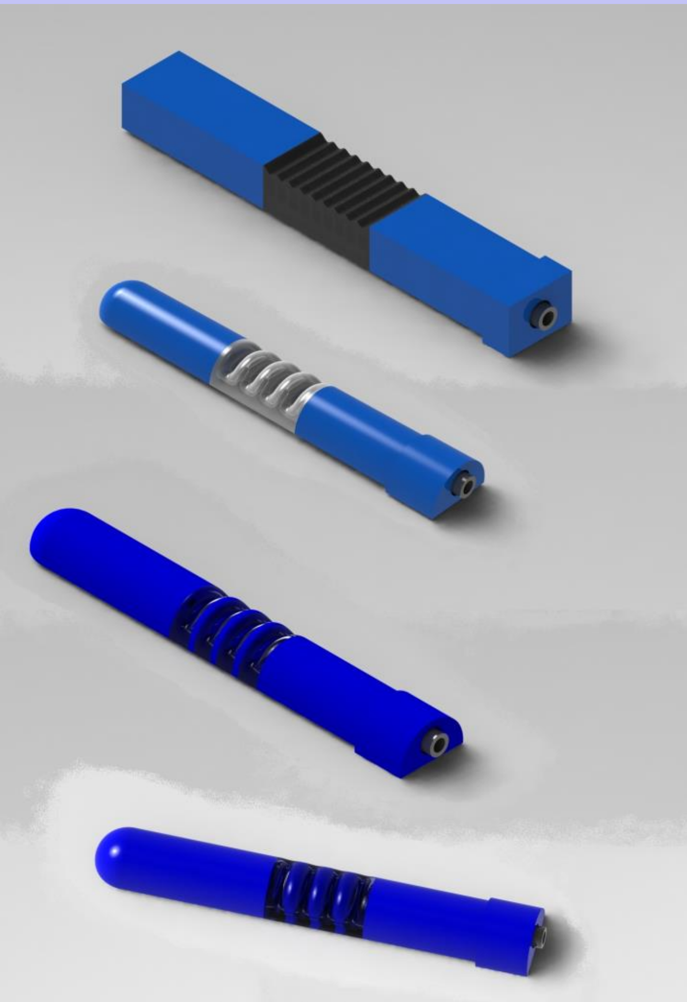

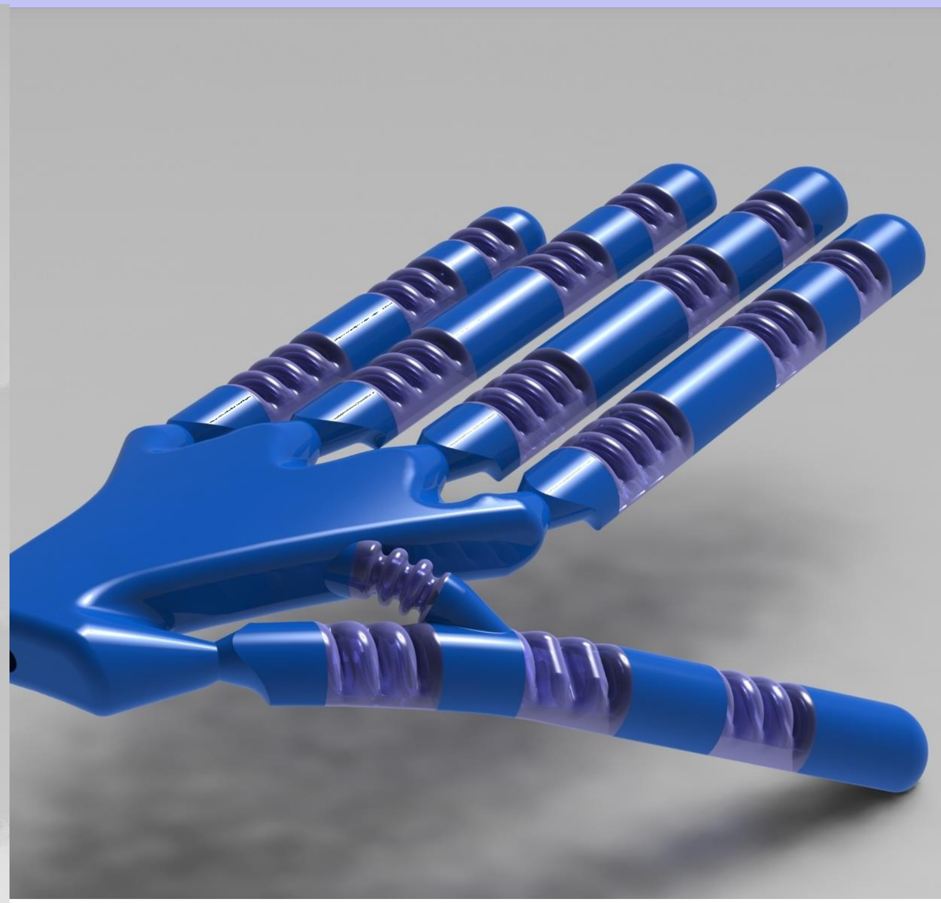

3D Printed Soft Fluidic Actuator for an Assistive Hand Exoskeleton Device

By

Koiliaris Panayiotis

in partial fulfilment of the requirements for the degree of

Master of Science
in Mechanical Engineering (Track: Biomechanical Design)

at the Delft University of Technology,
to be defended publicly on Wednesday January 31, 2018 at 10:00 AM.

Supervisor:	Prof. Dr.Ir. D.H. Plettenburg	
	Ir. R.A. Bos	
Thesis committee:	Prof.dr. F.C.T. van der Helm,	TU Delft
	Prof. Dr.Ir. D.H. Plettenburg,	TU Delft
	Dr.ir. J.F.L. Goosen (Hans),	TU Delft
	Ir. R.A. Bos,	TU Delft

3D Printed Soft Fluidic Actuator for an Assistive Hand Exoskeleton Device

Panayiotis Koiliaris, (P.Koiliaris@student.tudelft.nl, Student ID: 4516133)
Dept. of Mechanical Engineering – Delft University of Technology
Mekelweg 2, 2628 CD, Netherlands

***Abstract* – In the following study, a new concept of an assistive hand exoskeleton device for Duchenne muscular dystrophy (DMD) patients is presented. Due to the nature of this disease (causes progressive muscle degeneration from a young age of five years old), the requirements for such a device are very demanding, with extreme space and weight limitations, as well as high generated forces. The idea that is presented, is a 3D-printed soft hydraulic actuator that can be used to actuate such a demanding device. Different actuator prototypes have been prepared and tested, with a maximum generated force of around 0.4N. The outcome force does not fulfill the functional requirements that is 1-3N, but space, range of motion (ROM) and weight requirements have been met. In addition, the author demonstrates a complete design of a single-part, 3D-printed assistive hand exoskeleton device, with both the hydraulic circuit and the soft hydraulic actuators embedded in it. Despite the functional requirements that haven't been fulfilled, the idea of a single-part 3D-printed hand exoskeleton device is beneficial in simplicity, required space, cosmetic appearance, as well as the overall weight that was estimated to be no more than 150gr. Finally, there is a discussion regarding the future steps that the author suggests to increase the maximum generated force of the soft actuators and therefore the development of the first single-part, 3D-printed hand exoskeleton.**

***Index Terms* – Soft actuators, 3D printing, Hand exoskeleton, Duchenne muscular dystrophy.**

I. Introduction

Muscular dystrophy is a group of frequently occurring diseases that causes progressive weakness and muscle degeneration, resulting to the patient's limitations of motor functions [1]. According to the study of Monckton et al. 1982 [2], approximately 1 in 3500 of male births are suffering from this disorder, while more recent studies [3], show that for the year 2007, around 0.015% of 5-24 years old males in U.S. have been reported with a muscular dystrophy disorder (approximately 1 in 6800 of male births).

Duchenne muscular dystrophy or DMD, is a specific muscular dystrophy disorder caused by mutation of the DMD gene. The DMD gene is responsible for the production of a protein called dystrophin [4-5]. The exact relation of dystrophin and muscle degeneration is still unclear, however it is known that it is an X-linked disease, which affects mostly boys, while females are usually carriers and do not demonstrate any symptoms. DMD can cause severe loss of motor function, motor delay and abnormal gait, orthopaedic problems as well as cardiac and respiratory diseases [6-8]. Symptoms like difficulty of running or getting up, appear from the early age of three years old and steadily progress to muscle degeneration and motor function limitations, affecting first the lower extremities followed by the upper extremities. Full time sitting begins at the age of 12 and eventually fatality of cardiac and respiratory muscles appears by the late teens – early twenties [9-11]. Engineering an assistive device that can help those patients, to their early stage to be more self-dependent, is of a great importance and therefore the main focus of this study.

DMD can be characterized with five different stages [10]. The first stage is the diagnostic stage and concerns patients of 0-5 years old. At this stage, delayed walking is observed (18-24 months) and as the patient grows older (4-5 years old) demonstrates an inability to keep up with his peers. In addition, the patient rises from the floor using Gowers maneuver, due to proximal weakness of lower extremities [9-10]. Between the ages of 5 to 8 years old, that is the second stage, the symptoms are more obvious with advanced lower extremity limitations. Problems with running and walking up and down stairs developed, forcing the patients to use their upper extremities by using handrails for stability and additional strength [9].

Stage 3 appears at the age of nine and is followed by stage 4 at the age of 12. At those two stages, the patients gait abnormality increases and critical spinal deformity appears. In combination with easy fatigue and progressive weakening of quadriceps muscles, the patient begins full-time sitting [6]. He relies even more to his upper extremities for prop and stabilization, as well as, relief of discomfort. Advanced difficulties performing daily living activities, resorts to the need of full-time assistance. At the age of 16 the patient enters the final and most critical stage. Restrictions to both, upper and lower extremities increase, leading to the inability of feeding themselves and to difficulties controlling a standard joystick [9].

Even though some therapies are underdeveloped, there is no treatment for DMD. Corticosteroids tend to slow down the effects so they are provided to the patients, but that leads to obesity [10]. In addition, patients follow rehabilitation programs to maintain their mobility [9]. From an engineer's perspective, the research focused on the development of exoskeleton devices for both rehabilitation and assistive purposes. Existing exoskeleton devices are specifically designed for rehabilitation of a specific part of human body (i.e. shoulder, elbow, hand exoskeleton devices). Those exoskeletons, often tend to be bulky, uncomfortable and/or stationary. Ideally for rehabilitation purposes, and the only option for dystrophy patients, is to have a portable exoskeleton system, which is lightweight, affordable, easily wearable and cosmetically presentable. Portable or stand-alone exoskeleton devices have very demanding specifications due to the combination of: allowable weight, free space and important functions that the exoskeleton should fulfill. Those specifications are well described later on (see Section III).

Another huge advantage of a portable exoskeleton is that it can also be used as an assisting device. Even if the nervous system of muscular dystrophy patients is affected at the most advanced stage [6,12], the use of hand exoskeleton systems fed with the electromyography (EMG) signals of hand muscles, can provide a significant movement assist and quality of life improvement for the earlier stages. A portable hand exoskeleton assisting device will empower the upper extremities of the patient, allowing him to be more self-reliable for daily living activities. In addition, it will give the patient the additional strength that he needs at the stage 3 and 4 for self-stabilization, as well as the possibility for home-rehabilitation.

The focus of this research is: *the development of a hydraulic actuator that can be used in a portable exoskeleton device for Duchenne muscular dystrophy patient.*

Hydraulics and pneumatics have a high power to weight ratio and the potential to fulfill the demanding requirements of a portable hand exoskeleton system [13]. Even so, they are barely used for that purpose due to their complexity, expensiveness and difficulty of miniaturizing all the different components [14]. Researchers are focused on developing small hydraulic actuators that can be used for that purpose as well as other possible uses. Some interesting studies are discussed later on (see Section IV). In this study the use of a 3D printer for the development of such an actuator, is a subject of high interest. Two different printing technics for printing a soft hydraulic actuator, are investigated and compared. By successfully developing a 3D printed miniaturized soft hydraulic actuator, will eventually lead to the construction of a single-part 3D-printed hand exoskeleton device.

Being able to simply 3D print the whole exoskeleton device and have it ready for use is beneficial in many ways. First of all the cost will be minimized to affordable levels. The discretion and the simplicity of use of such a device will encourage the patients to use it for both all day assisting and rehabilitation purposes. From the production point of view, the hand exoskeleton device, as a single part, could easily be parameterized and quickly adapted to any patient. The feasibility of such a device is also discussed in this study and a conceptual design is presented by the end of it, for future research and development.

In the following Section the problem is analyzed, while in Section III, the requirements for the exoskeleton system are presented. In Section IV, some related studies are summarized. The design and development procedure of a 3D-printed soft fluidic actuator, as well as the testing methods are explained in Section V and the results are analyzed in the follow-up Section. The design of a single-part, 3D-printed hand exoskeleton device is presented and discussed in Section VII. Finally, the results are presented in Section IIX while conclusions are discussed in Section IX and some tips for future work are given in Section X.

II. Problem Analysis

In this study, we investigate the opportunity of developing a portable, assisting hand exoskeleton device for Duchenne patients, which will be suitable, affordable, easy to use and comfortable for them. From an engineer's perspective, this is a huge challenge. Among other requirements that will be analyzed in the following section, the biggest challenge is the size of such a device. In combination with the maximum weight and the functionality that such an exoskeleton must have, the engineer's options are minimized. Fortunately, recent evolution of the 3D printing technology opens a whole new area of research and gives the opportunity to be used as the missing piece of the puzzle for solving the problem.

The research of MacCurdy et al. [15] is a recent example, which demonstrates the capabilities of 3D-printing technology. By successfully creating a miniaturized hydraulic actuator that is ready for use, by using only a 3D-printer, also points out to the direction of combining hydraulic power with the newly developed 3D-printing technology. Previous studies [13], have shown that pneumatics and hydraulics can be very lightweight with some of the highest power density ratios (5 × 106 Wm-3 and 5 × 108 Wm-3 respectively), compared to other technologies. That means, they are the most promising technologies for miniaturizing and still be capable of producing a significant amount of force. Combining those two pieces of information, the idea of a single-part, 3D-printed hand exoskeleton device rises.

For such a device to exist, the feasibility for a 3D-printed actuator that is small enough and still be able to empower the

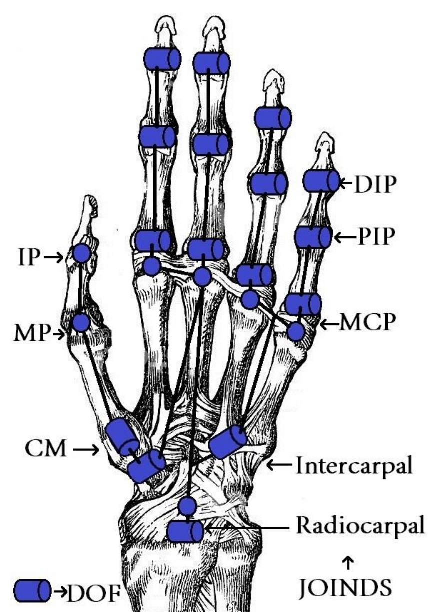

Fig. 1: Bone anatomy of a human hand, with indication of the joints and theDOFs [17].

exoskeleton is investigated. Some prototypes have been developed, analyzed and compared (see Section IV). The prototype soft hydraulic actuators, have been designed and developed such as to fulfill the most essential requirement; being able to be combined with a 3D-printed, micro-hydraulic circuit. Finally, an early design of a single-part 3D-printed hand exoskeleton is presented and discussed.

III. Requirements

For the design of an actuator for a hand exoskeleton device and eventually the device itself, several requirements must be taken into account. The direct link to the hand, the limited available space and weight of the device as well as the complexity of the hand itself, pushes those requirements to their extreme, limiting the available solutions for the designer [16]. For the purpose of this study, the requirements are stated and analyzed one by one, taking into consideration that the device is meant for DMD patients at the stage 3 and 4.

A. Degrees of Freedom (DOFs)

The need of clarifying the basics of hand anatomy and biomechanics is essential to ensure patients safety. First, despite the small space, a human hand has 23 DOFs, which are determined in fig. 1. Each finger has 4 DOFs concluding to 20 only on the fingers, 2 on the wrist and one on the metacarpal bones (see fig. 1) [17-18]. To encounter this problem, since it is very hard (if not impossible) to have a hand exoskeleton with 23 DOFs and still be portable and appealing, only the most important ones are adapted. Which DOFs are adapted to the exoskeleton, depends on the purpose of the device, but also on how complicated and how expensive it will be engineered. It is of great importance to realize that not each DOF needs an actuator. According to the design, number and complexity of grip motions that are needed (Favetto et al. [17], demonstrates the eight fundamental grips), one actuator can be used to activate several DOFs. Also, taking advantage of the fact that by definition the device is constrained by the patient's hand, redundancy of DOFs can be used. For this study, the goal is to mechanically activate 3 of the 4 DOF of the fingers, giving to the patient additional power for flexing and extending them. For abduction and adduction of the fingers, is not important to give mechanical support, but according to previous study [19-20], patients prefer to have some freedom for those DOFs. Taking that into account, besides the activation of the 3 DOF for each finger, the design of the hand exoskeleton must allow passive movement, coming from the patient himself.

B. Weight

An emphasis has been given to the DOFs, and that is because they have a great influence on other requirements like the weight. According to Aubin et al. [21], the weight that is being barge onto a patient's hand with grasp pathologies, from a robotic hand exoskeleton device, should not exceed 0.5 kg. Taking into consideration that for this study, DMD patients are

Fig. 2: Top: Soft actuated hand exoskeleton by Polygerinos et al. [24], bottom: hand rehabilitation exoskeleton device by Wege et al. [26].

the target group; that number has to be minimized even further, with the optimum to have a device with passive support, similar to Kooren et al. study [22]. For a non-passive support exoskeletons though, additional actuators result to extra weight.

Hydraulic or pneumatic systems are beneficial for that requirement because they have the advantage of planting the other components elsewhere and connect them with flexible tubes. Using that technic, a lightweight glove exoskeleton can be designed, to be comfortable for the user [23]. Nevertheless, an ideal solution is to have all components packed onto the exoskeleton device. That will give the simplicity of use to the patient, as well as the freedom from connection tubes and/or cables, converting that exoskeleton to a suitable and an everyday use device for DMD patients.

C. Space

Space availability, as discussed before, is another crucial requirement. When talking about a portable assisting exoskeleton device that will be used by the patient for everyday tasks fitting it onto the wearer's hand is not always enough. In some cases, researchers are either more tolerant or fail to fulfill this requirement, resulting to a bulky hand exoskeleton. Of course the functionality is very important, but if the purpose of the device is for self-rehabilitation and everyday use, the patient will prefer a more compact and attractive one. Fig. 2 demonstrates the difference of the appearance between two hand exoskeleton devices, both designed for rehabilitation purposes but design and actuation choices differ (Polygerinos et al. [24], top and Wege et al. [25-26], bottom). It is obvious that a simple looking hand exoskeleton device is more appropriate for both rehabilitation and assisting purposes. From a user study that took place in previous research (and concerned stroke patients) [19-20], it was found that cosmetic appearance is as important as the functionality of such a device.

Using DINED anthropometric database [27] the index finger of a male adult has an average length of 75 mm and a diameter of 15 mm. Combining that information with the age of the target group (9-16 years old), those numbers can be safely assumed to be even smaller. From the same database [27], it is found that the average length of a 9 year old child's middle finger, is 64 mm. That limits the space availability even further, resulting to miniaturization restrictions (additional information are presented in Appendix I).

D. Safety

It has been stated earlier that realizing the biomechanics of human hand is essential for the wearer's safety as well as that a hand exoskeleton device interacts with the human directly. Two important points that have to be analyzed to reinsure the safety of use of such a device. Biomechanics of human hand, can give to the researcher the range of motion of each joint. Therefore, limitations on the range of motion of the device, i.e. using mechanical stoppers, must be adapted, in a way to not exceed the natural, human, range of motion and prevent self-injuries.

The second point can become more complicated. Since this study is dedicated to investigating the use of fluidics for the actuation of a hand exoskeleton, supplementary safety measurements must be taken into consideration. Any malfunction to a component with a high internal pressure, can cause serious damage to the patient. A malfunction to a pneumatic component, due to high gas compressibility, can result to a violent release of the system's internal pressure, compromising the safety of the patient. On the other hand, a malfunction to a hydraulic component is less violent due to lower working pressures and incompressibility of fluids, but it can still be harmful to the wearer (i.e. working fluid could get warm due to friction, and when a leakage appears might harm wearer's skin). Safety valves are designed to reinsure that the pressure of the system will not exceed a specified limit, but that might not be enough. Designers have to be very thorough with their designs and be sure that if a malfunction appears, injuries could still be avoided. For example, that can be achieved by appropriately designing the weak points of the device, opposing the interaction points with the hand of the patient. Also, when a hydraulic system is applied, the liquid selection is important. Even if it is proven that the system is leakage-free, no acidic or basic liquids or liquids that may cause allergic reactions (according to the wearer) must be used. Last but not least, the center of rotation of the device must coincide with the center of rotation of the user's joints [28] or to adapt a remote center of rotation [29-30]. If that's not true, a conflict between the exoskeleton and the wearer will occur, concluding to injuries.

E. Functionality

For the device to be practical and function correctly, it must be able to generate a desirable force and work with a specific speed to achieve natural motion. In the means of a fluidic system, this translates to the pressure of the system, as well as the flow rate of the fluid (either gas or liquid) and the desirable actuation stroke (which depends on the range of motion that needs to be achieved and the design of the system). Furthermore, the pressure and flow rate also depends on the system that is to be designed; meaning that, different pressure ranges apply for: a master-slave system or a pump system, a soft actuated system (i.e. flexible hydraulic/pneumatic actuators, artificial rubber muscles) or a hard actuated system (i.e. hydraulic/pneumatic cylinders). Previous studies indicate a variety of desirable forces. Matheus et al. [31] demonstrates that daily living objects do not weight more than 1.5 kg, and Polygerinos et al. [23-24] translated this information into 7.3 N tip force using a friction coefficient of 0.255. Smaby et al. [32] identified the key pinch forces required for daily activities, to range from 1.4 N (push a button) to 31.4 N (insert a plug). Other studies that concern hand exoskeletons as well as prosthetics, seem to agree with those numbers, concluding with devices that are able to obtain 3-8 N of fingertip force [33-36]. However, those forces do not indicate the required force needed by the actuator since, for example, the actuator itself can be used with a leaver system. Different tasks involve different number of fingers as well as different grasping patterns. According to the design and the number of actuation that the device will have, those forces could be used as a reference, but the actuation force required, will differ.

The speed of the actuation cycle, also depends on the purpose of the device. If the purpose is to assist patients with muscular disorder, the actuation needs to be fast enough for the resulting motion to look natural. On the other hand, if the exoskeleton is designed for rehabilitation exercises, then the actuation speed and frequency must be related to those exercises. For the case of this study, the need for assistance is of a major importance, but combining it with the need of rehabilitation will optimize the exoskeletons functionality. According to Polygerinos et al. [24] a frequency of 0.5 Hz for finger flexion/extension, is sufficient for both purposes. On the contrary, Schulz et al. [34] designed a hand prosthesis able to operate ten times faster than that (a frequency of 5 Hz) resulting to more natural movement.

According to that information, it can be concluded that it is hard to set a specific pressure or flow rate as a requirement. This is also confirmed just by looking at the variety of different pressures used in different studies; hydraulic systems operating with pressure ranging from 0.5 bar to 250 bar [14, 23-24, 35-39] and pneumatic systems, from 0.2 bar to 12 bar [33, 40-43]. On the other hand, taking into account the mechanical design of the device, the working pressure and flow rate of the device must be adjusted such as the device can give enough additional energy to the patient.

F. Range of Motion

The range of motion (ROM) of the fingers, is not only involved with the safety requirements but is also related to the desirable stroke of the actuator when it is attached to the actuation point. According to Hume et al. [44], the ROM of the

Fig. 3: MacCurdys' 3D-printed bellow produced as a single part with pre-filled with printable liquid internal channels [15].

four fingers MCP joints is 0º – 100º, for the PIP joints 0º – 105º and for the DIP joints 0º – 85º. For the thumb those numbers differ, with the thump's MCP joint to have a ROM of 0º – 56º and the IP joint -5º – 73º. Once again, those numbers do not directly translate to stroke. First of all, as Hume et al. [44] mentioned, the functional ROM (meaning the ROM that is used for daily living activities) differ. On their study they measured the ROM of 11 daily activities and they found the following average ROM for the thumb: MCP: 10º – 32º, IP: 2º – 43º, and for the four fingers: MCP: 33º – 73º, PIP: 36º – 86º and for the DIP: 20º – 61º. With that information, someone can choose to implement the functional ROM on an assisting exoskeleton device instead of the actual ROM of the finger. In addition, the displacement of the actuator(s), for the fingers to achieve that ROM, depends on the design of the exoskeleton as well as, the type of actuators that will be used (i.e. artificial muscles or cylinders).

For the purpose of this study, some compromises, as well as some priorities on requirement fulfillment have been set. Starting with the space availability, the actuators for the exoskeleton as well as the device itself, will be designed assuming hand dimensions of a male adult. The feasibility and technological limitations for miniaturizing even further (adapt to a child's hand), is discussed at Section IX. In addition, greater importance is set for the easy usage, patient's comfort and safety, as well as the cost, weight, functionality and adaptability of the device.

IV. Related Work

Even though 3D-printed hand exoskeletons and miniaturized hydraulic actuators are new concepts, multiple studies already exist. Some of those studies are reviewed in this section, and a summary of them is presented. It has been evaluated whether their technologies or techniques could be used for an elegant design of a hand exoskeleton device. Additional information about 3D-printing technologies can be found in Appendix II.

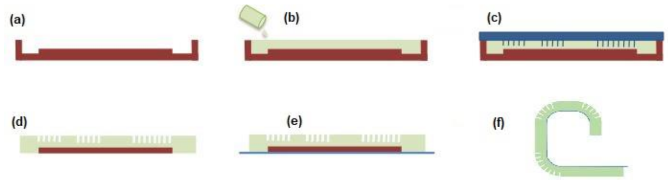

Fig. 4: Fabrication process of Yap et al. actuator, a) Mold, b) Pour liquid elastomer, c) Feature mold for creating variable stiffness at different localities, d) Cure at 60 ºC, e) Seal the bottom with strain restraining fabric, f) Bending motion of the actuator [46].

One of the most recent examples is the impressive work from MacCurdy et al. [15] who introduced a new way to develop a hydraulic actuator. They used an MJP (Multi Jet Printing) printer to 3D-print a hydraulic below, with selectively different stiffness at specified areas for optimum functionality. In addition, MacCurdys group adjusted the printer such as to print water as a secondary support material. Using this modification, they manage to benefit from the disadvantage of that printing technology. Cleaning the printed part from its support material, limits the minimum dimensions that an inner structure can have, therefore scaling down a hydraulic part is also limited. On the other hand, printing water or other liquid as a support for an inner structure, gave them the opportunity to 3D-print a miniaturized, fully functional, pre-filled with water hydraulic below that is ready for use (demonstrated in fig. 3). Furthermore, by the end of their study, they demonstrated that using this method, a fully functional hydraulically actuated robot that is printed as a single part is possible.

A totally different concept is represented by Yap et al. [45-47], on their studies on soft, pneumatically actuated, hand exoskeleton glove (ExoGlove). They designed molds for the fingers of the exoskeleton device, giving them the opportunity to use liquid elastomer for the creation of flexible parts. In addition, the design has been prepared having different thickness, such as to result to variable stiffness. By attaching soft pneumatic actuator at the bottom, they achieved the required range of motion (see fig. 4). Using this technique, they manage to create a fully functional and compact ExoGlove that can produce an acceptable passive force of around 3.5 N. At their latest study [47], they optimized their design and they tried different materials. They successfully achieved forces of around 10N (with Dragon Skin 20-Medium). The control system and the compressor (or miniature diaphragm pump)

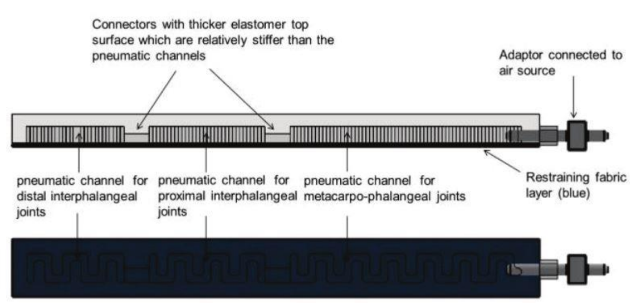

Fig. 5: The soft finger actuator with pneumatic channels by Low et al. [48].

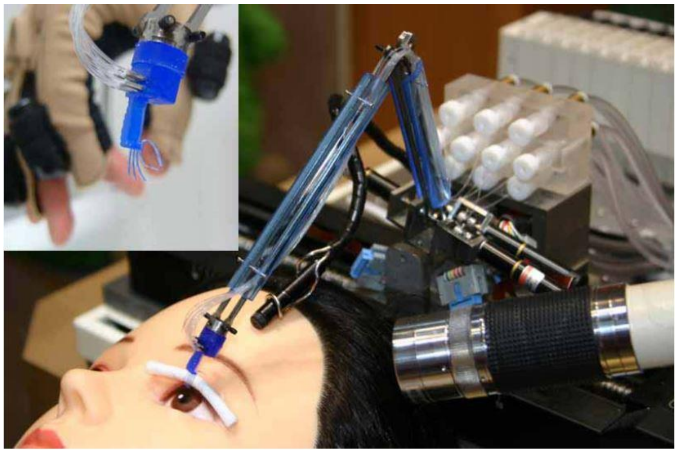

Fig. 6: Micro manipulation robot system by Konishi et al. [49].

have been placed separately from the glove, optimizing its weight and size.

Similarly, Low et al. [48] also used molds to develop soft fingers for a prosthetic and/or an orthotic device. Dragon Skin 10-Medium was the chosen material, since it combines hyper-elastic properties (maximum strain up to 1000%) and acceptable stiffness for the purpose of their study. A totally different design than Yap et al. is been used though. Their idea was to create an inner pneumatic main channel that connects the 3 differently shaped channels with lower thickness hence different stiffness, together (fig. 5). With their unique design and input pressure of 1 bar, they manage to achieve the desirable range of motion in addition to the 2N of force per finger. An important part of their study is that by succeeding in creating functional pneumatic actuators out of molds, they gave access to a whole new area of research that still needs to be exploit.

An impressive pneumatic micro-hand is presented by Konishi et al. on their study, back in 2006 [49]. Very similar to the previously analyzed study of Low et al., they used molds to create an inner pneumatic circuit and variable thicknesses at the actuation points to create balloon type actuators. The innovation of this study is the size of the hand that can be established at the microscale. They used Polydimethylsiloxane (or PDMS) as the main material and the micro-hand functions as a slave system. In fig. 6 the scale of the device can be realized, as well as a possible application of such a system.

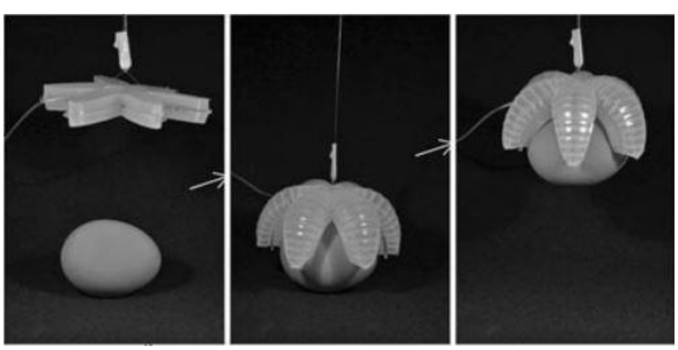

Fig. 7: The PneuNet by Ilievski et al. [50], gripping an uncooked chicken egg.

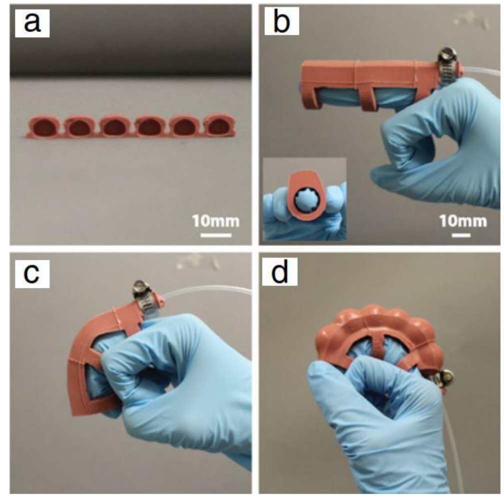

Fig. 8: (a) Rotationally cast, pneumatic network monolith, (b) encapsulated into exoskeleton form and placed on a finger, (c) uninflated finger actuator bends with finger and (d) inflated finger actuator (by Zhao et al. [51]).

Adapting similar, balloon type pneumatic actuators in bigger scale, both Ilievski et al. [50] and Zhao et al. [51] manage to develop finger-like devices; the former for gripping robotic limb (fig. 7) and the latter for exoskeleton applications (fig. 8). For the materials used, Ilievski et al. used a combination of Ecoflex and PDMS for more stable motion, while Zhao et al. tried both Ecoflex and Elastosil. They manage to successfully create forces of 3N and 27.4N respectively. The difference between the results of the two studies are due to different scaling (Ilievski et al. developed a much smaller device than Zhao et al.), as well as to the materials used and to the application that are made for.

Another concept of soft robotics is presented by Scharff et al. [52]. In his study, he manages to develop a hand prosthesis that is pneumatically actuated. The innovation of his study is that he used soft pneumatic actuators that they have been embedded in the prosthetic hand itself, allowing him to 3D-print the whole prosthetic hand as a single part. Scharff, used Selective Laser Sintering (or SLS) printing technology and a thermoplastic polyurethane (TPU) as a working material, due to its balanced flexibility and stiffness. An external pneumatic circuit has been adapted for the functionality of the prototype that is demonstrated in fig. 9. The prototype is made for hand-shaking, which uses the soft pneumatic actuators to identify the force that is applied to it and respond accordingly. Scharff's study demonstrates: a) the possibility to use SLS printing technology to 3D-print hand prosthesis as a single part with all its actuators embedded in it and b) the use of soft robotics for human-Robot Interaction (HRI).

Finally Rus D. and Tolley T.M. gave an analytical review on soft robots [53]. This review is not going to be analyzed in this study, but it is worth mentioning since it summarizes lots of interesting solutions for designing soft actuators; some of them adapted for pneumatics or hydraulics (Fig. 10 demonstrates some of those designs). For additional information, in Appendix III a summary of a literature review on miniaturized

Fig. 9: Scharff et al. soft robotic hand [52].

fluidic components for a hand exoskeleton, from the same author, is presented.

V. Actuator Design and Methods

All those studies, already proven the plausibility of the idea of a single part 3D-printed hand assisting exoskeleton that fulfills all the requirements (see requirements, Section III). But moving from the idea to the development of a prototype, a lot of problems must be solved. The actuation is the first piece of the puzzle, so the focus of the first part of this research, is on the design, development and test of a 3D-printed, soft, fluidic actuator that can be adapted on a hand assisting device for DMD patients. Printing a soft fluidic actuator has a couple of limitations. First, it must be printed with a soft material and soft materials are harder to print, and second it must have an inner structure. Inner structures need support and that limits the minimum size of the design, such that, support material can still be cleaned out.

MJP and SLS printing technologies were chosen as the most suitable ones for prototyping and testing the actuation. MJP technology uses liquid plastic to print and that is beneficial for print materials with specific stiffness (by mixing a soft material with a stiff material). In addition, due to the "liquid print" technique opens the opportunity to use a variety of support material such as water (see Section IV, MacCurdy et al. [15]). With that technique dimensional limitations for the inner structures are becoming lower, and in addition, the final products of such a printing technology have precision up to microns and have more isotropic characteristics than products from other printing technologies (e.g. Fused Deposition Modelin, or FDM) [54-56]. On the other hand, SLS printing uses powder as a material and a laser to melt and fuse it to create the product layer by layer. This technique allows to print in a variety of different materials; from plastics, to even soft metals such as aluminum. Another benefit of SLS technology, is that the powder itself is used as a support material and that makes the cleaning process much easier. Neither chemical solvents nor

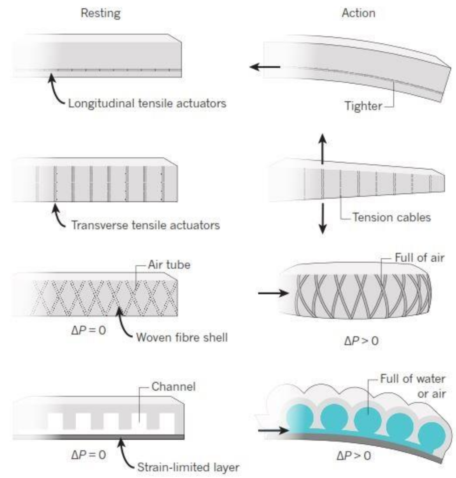

Fig. 10: Cross-section of common approaches to actuation of soft-robot bodies: in resting (left) and actuated (right) states, summarized by Rus D. and Tolley T.M. [53].

heating treatment is needed to extract the powder from an inner structure. Just by using compressed air, the supporting powder can be blown out [57]. A drawback for both printing technologies is that the 3D – printers are expensive to buy, but even so, companies from which you can order your 3D – product exist offering both MJP and/or SLS printings (e.g. Shapeways [58]). More information about printing technologies are presented in Appendix II.

At this point, it is important to mention that lots of different designs of soft actuators already exist and even more are meant to be developed; but it is very difficult, if not impossible, to accurately choose the best one. Running simulations is a good start to give a rough evaluation or compare some designs, but complex geometries can take a lot of hours to be solved and most of the times, results are far from reality. In this study, due to the complexity of the requirements, a new design of a soft fluidic actuator has been created based on previous studies. The first design was further modified and optimized through trials.

A. Design Procedure

Fig. 11 demonstrates the initial design and its cross-sectional area. As it was mentioned earlier, using MJP technology gives the opportunity to choose a specific stiffness and that allows to adjust two different stiffness to build up the part; the hard area that supports the actuator, and the soft area that will be the actuator itself (area c). The stiffness of the soft area is initially selected to be 70% stiff, while the hard area to 100% stiff. Since, according to author's knowledge (see Section IV), no previews studies used this technique for that purpose, the stiffness for the soft part is initially chosen randomly, but different stiffness are also tested at a later stage of the study. The rectangular shape and dimensions of the actuator (see fig. 11) allows the option of an easy adaptation on a hand exoskeleton while the inner structure allows the connection to a larger inner fluidic circuit. The shape of the actuation chamber is designed such that will allow a rotational motion when it's

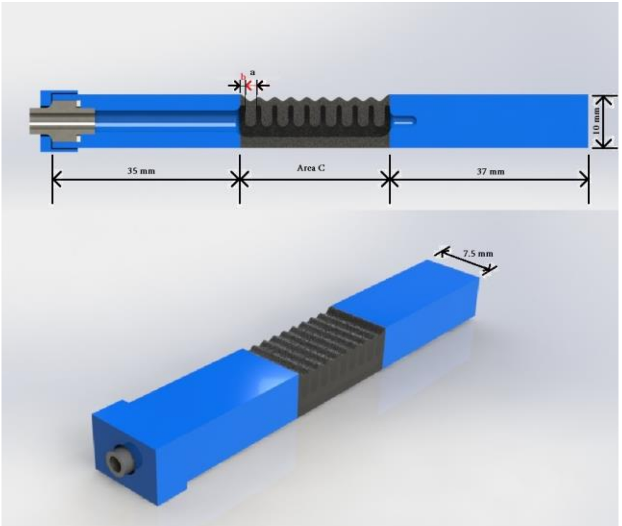

Fig. 11: Initial design and its cross-sectional area of a 3D-printable soft fluidic actuator. The height of the actuator is 10mm and its length and width are 28mm and 7.5mm respectively. The length varies according to the design.

under high pressure. Fig. 12 represents the displacement solution of a simulation that is prepared for functionality test and proof of design. The first prototype is tested using pressurized air. The material used for all the parts is FLX985 (Agilus 30 Black), RGD843 (VeroCyan) and RGD851 (VeroMagenta). The support material was extracted using a basic solution. The solution dissolved the support material out of the actuator, but due to the small openings accessing the inner chamber, cleaning process took several days for each part, resulting to the start of dissolution of the non-support, soft material. Nevertheless, the damage thought to be minimum, and the parts were used for further experimentation. It is important to mention that, same as the simulation, the first couple of designs have been experimented to proof the functionality of the actuator, as well as, to adapt the ROM.

Even though, the results demonstrated that the initial actuator was weak and failed at 1.2 bar of pressure, some observations are critical for the preparation of the second design. Fig. 13, shows the actuator under 1.2 bar of pressure. Two things can be observed: a) the range of motion is limited and b) the actuator was mostly swollen at the bottom rather than the upper area. To encounter those problems, dimensions a, c and the ratio a/b are

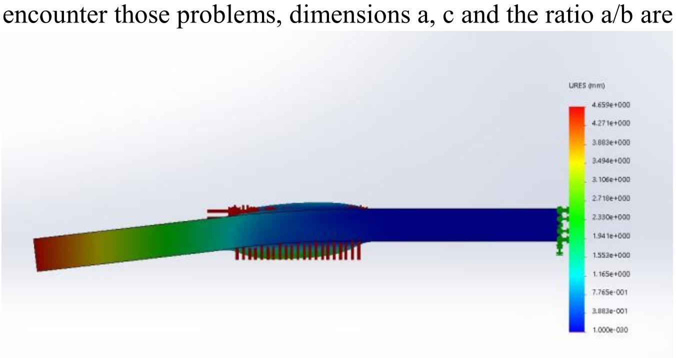

Fig. 12: Simulation of the first design when the internal chamber is under pressure (2 bar) and the right side is fixed. Results are not accurate due to simplifications, but functionality is proven.

Fig. 13: First prototype of a 3D-printed soft actuator with soft area (black material) adjusted to be 70% stiff while the hard area (blue material) to be 100% stiff. The actuator is under 1.2 bar of air pressure.

changed such as to separate the bigger chamber into multiple smaller ones. Doing that, the surface area of the upper part of the actuator increases, forcing it to rotate even further when is under pressure. In addition, an inner wall is adapted between each chamber. The change in thickness of the bottom layer of the actuator due to those walls, changes the stiffness at the direction of the walls, allowing to the designer to control the swollenness direction of the actuator when it's under pressure. Also, a circular shape is adapted for aesthetic reasons and is shown in fig. 14a.

Printing and testing the 2nd design with the same stiffness as the first one, allowed some adjustments to the design. Fig. 14b, demonstrates the actuator under 1.2 bar of pressure. It is obvious that the range of motion is increased, but, same as the 1st design, it failed at 1.2 bar. To minimize the swollenness when the actuator is under pressure, and therefore increase the maximum pressure that it can withstand, different solutions have been tried out. Reinforcement rings with different stiffness are designed along the length of the actuator as shown in fig. 15a. In other designs (fig. 15b), the reinforcement rings are placed between the chamber and the soft material (resulting to have half the wall thickness), to avoid failures due to weak points that are created to the bonding area of soft and stiff material. Four final designs with dimensional differences have been prepared and tested. In addition, the 3rd design was tested as a hydraulic actuator, using pressurized water. Having in mind that hydraulics have higher power-density ratio, the reasoning behind the test was to increase the outcome generated force using the same pressure.

To have a complete overview on the capabilities of MJP technology, the 3rd design was also prepared with 3 different stiffness of the soft material; 60%, 70% and 85% stiff. The stiffness was chosen according to the choices that the printer allowed. Using this approach, after the analysis of the results, the most suitable stiffness for our application can be chosen. Table I represents the characteristics of the designs.

Finally, the design was adjusted for SLS printing (fig. 16) and printed from the company Shapeways using an elasto-plastic material [58]. In this case, the overall dimensions are larger, due to printing requirements for the cleaning process (characteristics are also shown in Table I). Nevertheless, it still fulfills the requirements for the desirable actuator.

TABLE I
SUMMARIZE OF THE CHARACTERISTICS OF ALL DIFFERENT DESIGNS

Design	Length of C [mm]	a [mm]	Ratio: a/b	# of Chambers	Internal Wall			Reinforcement Rings		
					#	Thickness [mm]	Height [mm]	#	Width [mm]	Thickness
1st	28	3	3	1	-	-	-	-	-	
2nd	25.25	5.75	2.556	5	3	0.75	3.5	-	-	
3rd	25.25	5.75	2.556	5	3	0.75	3.5	3	1.5	Wall thickness
4th	25.25	5.75	2.556	5	3	0.75	3.5	3	2	Wall thickness / 2
5th	25.25	5.75	2.556	5	3	0.75	3.5	4	2.25	Wall thickness
6th	25.25	5.75	2.556	5	3	0.75	3.5	4	2	Wall thickness / 2
7th				Same as 3rd design, printed with 60% stiff soft material						
8th				Same as 3rd design, printed with 60% stiff soft material						
SLS	30	8.375	1.718	4	2	0.875	4	-	-	-

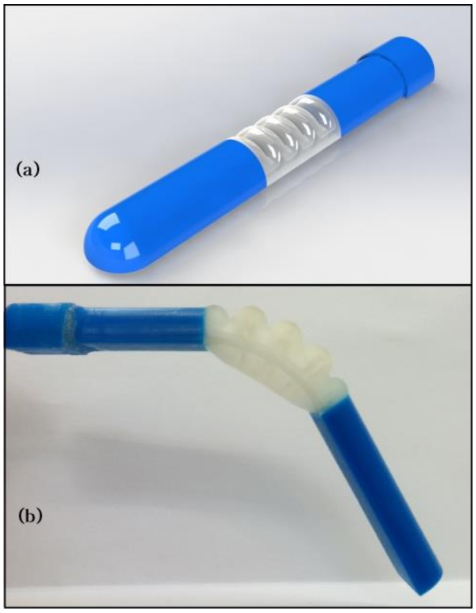

Fig. 14: Second trial: a) design with adjusted a and b dimensions. Circular shape was adapted and b) the real actuator under 1.2 bar of air pressure.

B. Testing Procedure

Excluding the first two designs, the other parts were tested for: maximum allowable pressure, range of motion in different pressures and generated force at the tip of the part (corresponds to the fingertip). Those measurements are important since all three are correlated with each other but they are also highly dependent on the design and the stiffness of the material. The testing configuration is demonstrated in fig. 17. As it can be seen, the part is placed to the main base that fixes its bottom area. The actuator (soft area) is kept free, while the upper area of the part pushes a piezoelectric force sensor (name of force sensor) allowing the measurement of the generated forces. The force sensor is connected to an arc that locks every 5 degrees, starting from a straight position. It allows a ROM of 115 degrees that is larger than the maximum required one, giving the possibility to measure the ROM of the actuator at different pressures with the accuracy of 5 degrees, as well as the generated force at different angles.

A LabVIEW program has been used to gather the data of the experiments. Using a FESTO air pressure regulator (Festo

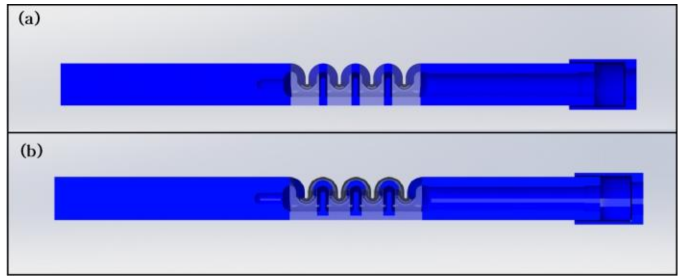

Fig. 15: Cross-sectional areas of the designs of soft actuators with reinforcement rings adapted to them: a) The wall thickness of the rings is the same with the wall thickness of the structure and b) the wall thickness of the ring is half the wall thickness of the structure, allowing them to be in-between a single part of soft material, minimizing the weak points of the actuator.

MS4-LFR 5μm G 1/4 Filter Regulator), samples were taken with the pressure initially set to 0.5 and 1 bar. After 1 bar, pressure increment rate was set to 0.2 bar. All the data are presented in Appendix IV and the results are analyzed in the following Section.

VI. RESULTS AND COMPARISON

For the analysis of the data, surface plots have been prepared (fig. 18-20). The 3 dimensional plots represent to the X-axis the curvature of the actuator in degrees (or ROM of the design pressurized with the corresponding pressure), to the Y-axis the pressure in bar and to the Z-axis the generated force in Newton. It is worth mentioning that the experiments were none reversible, since the maximum pressure and ROM were investigated. That means that the pressure was increased up to the failure point of each design. In addition, the extracted data

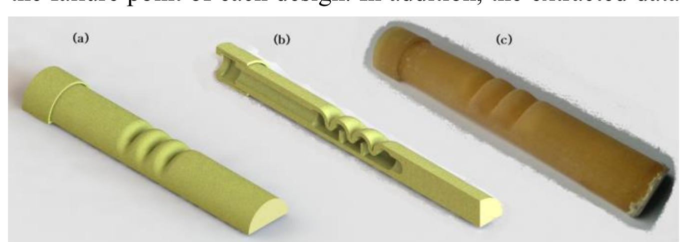

Fig. 16: a) Design of a soft actuator for SLS printing, b) cross-sectional area. Dimensions have been increased according to the specifications of the printer (for the powder material to be able to be cleaned from the inner structure) and c) the actuator printed from an elasto-plastic powdered material using an SLS printer by Shapeways.

Fig. 17: Testing configuration. Pressurized air is fed to the actuator, while the force sensor measures the force that the actuator is generating at the tip. The main base have a rotational locking system every 5 degrees (arc) allowing to also test a second feature: the ROM, with accuracy of 5º.

only give specific points on a 3D plot, but a linear relation between those points was assumed. The impact of this assumption is minimized by increasing the sampling rate and its benefit is that it can be used to create surface plots for better representation of the results.

The plotted surfaces represent the area of: pressure, ROM and generated force, which is allowed for the corresponding designs. Three different sets of surface plots have been prepared: fig. 18 compares the four different designs (3rd: 3 reinforcement rings with full wall thickness (3RRFT), 4th: 3 reinforcement rings with half the wall thickness (3RRHT), 5th: 4 reinforcement rings with full wall thickness (4RRFT) and 6th: 4 reinforcement rings with half the wall thickness (4RRHT)), fig. 19 compares the three different stiffness (3rd: 70% stiff, 7th: 60% stiff and 8th: 85% stiff) and fig. 20 compares water pressurization with air pressurization (3rd design). In addition, Table II, summarizes the maximum pressure, ROM and generated force at 0º and at 85º for all the designs. The 85º have been chosen since it's the maximum functional ROM that is required. Some of the data in that table are missing, meaning that they were not obtained (1st and 2nd design) or they didn't reach the required ROM resulting to 0N generated force.

TABLE II
SUMMARIZED OUTCOME RESULTS FOR ALL DESIGNS

Design #	Max.Pressure [bar]	Max. ROM [deg]	Max. Force @ 0º [N]	Max. Force @ 85º [N]
1st	1.2	15	-	-
2nd	1.2	65	-	-
3RRFT 70%	1.4	100	0.175	0.023
3RRHT 70%	1.8	65	0.21	-
4RRFT 70%	2.4	55	0.269	-
4RRHT 70%	2	35	0.21	-
3RRFT 60%	1.4	90	0.175	0.012
3RRFT 85%	2	75	0.316	-
Hydraulic	3	85	0.397	0.023
SLS	7	0	-	

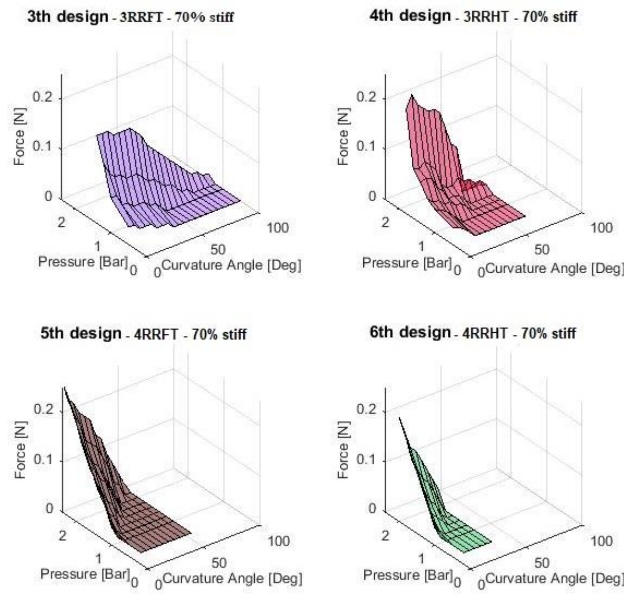

Fig. 18: Surface plots for the results of the four designs with reinforcement rings. X-axis: ROM (or the maximum curvature angle of the actuator when is under pressure), Y-axis: applied air pressure and Z-axis: generated force.

Overall, the outcome results cannot support the requirements for an assisting exoskeleton device. Even though the required ROM can be achieved, the maximum pressure that the actuator can withstand is too low, resulting to small generated force. In addition, the maximum force is generated at zero degrees, which means that at the maximum ROM the generated force is much smaller and very close to zero. According to the requirements, the actuator should ideally be able to generate minimum 1N of force (since the designs allow three actuators per finger, the net force will be 3N at the finger-tip), when it reaches the maximum functional ROM that is around 85º (see Section III). Compare to the maximum generated force at 85º from the tested designs (3rd design and hydraulically tested with 0.023N), it's almost 50 times larger. Some major factors, like the support material cleaning process and the weak points created at the bonding area of the soft and stiff material, were involved to the outcome of those results. Those two factors are further analyzed in Section IX.

Nevertheless, for MJP parts, the support material cleaning process was the same for all the designs, allowing the comparison between different designs even with small generated forces. Doing so, a wider overview of the different designs and the material properties of MJP technology can be obtained, leading to some conclusions for future studies. In addition, testing and comparing the pneumatic and hydraulic actuator as well as two different printing techniques, also gives some conclusions about their differences, and some ideas on how to proceed for the design of a better and more suitable actuator.

A. Reinforcement Rings Effect

According to the results, the 5th (4RRFT) and 6th (4RRHT) designs demonstrated more tolerance to higher pressures than

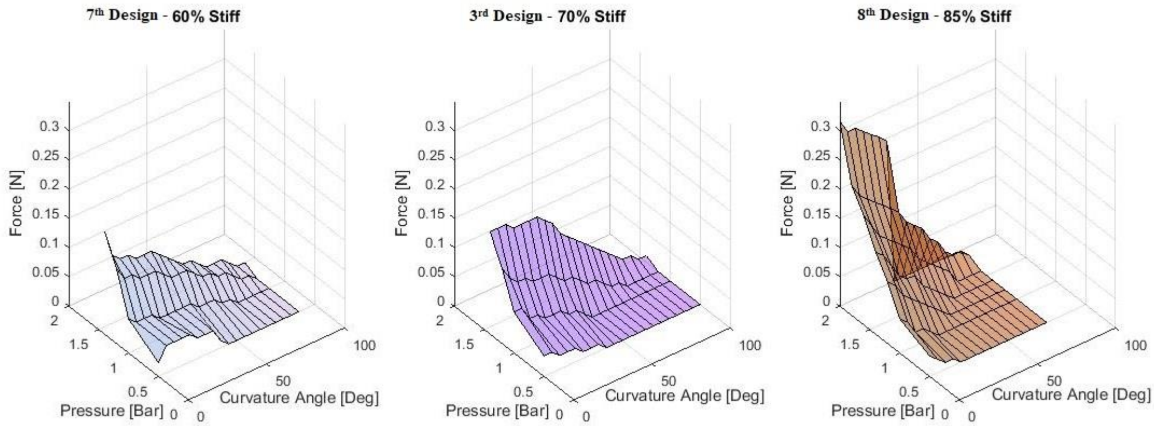

Fig. 19: Surface plots for the results of the same design printed in three different stiffness: 60%, 70% and 85%. X-axis: ROM (or the maximum curvature angle of the actuator when is under pressure), Y-axis: applied air pressure and Z-axis: generated force.

the 3rd (4RRFT) and 4th (4RRHT) design. As it can be seen from Table I, the 5th and 6th designs have thicker reinforcement rings, resulting to larger stiffer areas and smaller soft areas. Using this technique, the actuator was able to withstand higher pressures with the exchange of the ROM. The 3rd design proved to have the higher ROM, as well as the higher maximum force at the maximum functional ROM (even if it was very small). Of course, that alone cannot support the requirements for an assisting device, so a balance between the ROM and the generated force must be achieved such that could fulfill both the functional and the ROM requirements.

According to the four designs shown in fig. 18, even if the ROM was adjusted to be exactly as the maximum functional ROM (that is 85^o), the actuator would still not be able to generate enough force to support the exoskeleton. The third design as the most promising one, was re-printed using different stiffness for the soft material (60% and 85% stiff), as it was stated at Section V.

B. Comparison between Different Stiffness

Fig. 19 represent the results for the three stiffness. Same as before, there is a trade of between the maximum generated force and the maximum pressure that the actuators can withstand. Stiffer soft material results to higher pressures but the ROM is minimized. The effect on the ROM though is much smaller compare to changing the thickness of the reinforcement rings. The ROM of the 85%-stiff part was 75^o that is comparable to the 85^o of the maximum functional ROM, while the allowable pressure was almost 1.5X, larger than the 70%-stiff part. Between the 60%-stiff and 70%-stiff the differences are slim, but the 70%-stiff part demonstrated higher maximum force at 85^o.

Those results suggest that the best stiffness for the soft material is between 70% and 85% with the ideal one closing to 80%. Unfortunately, that was not an option due to printer limitations.

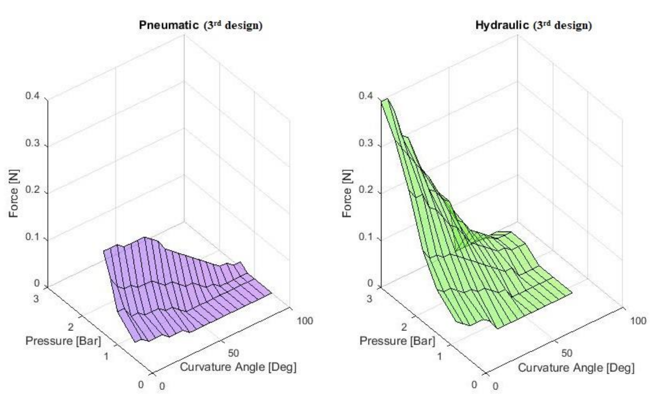

Fig. 20: Surface plots for the results of the same design, tested with pressurized air (left) and pressurized water (right). X-axis: ROM (or the maximum curvature angle of the actuator when is under pressure), Y-axis: applied air pressure and Z-axis: generated force.

C. Comparison between Pneumatic and Hydraulic Actuator

The results demonstrate that pressurization with water instead of air could generate higher forces (fig. 20). The ROM is lower but still meets the criteria of the functional ROM. Even though 85^o is its maximum ROM (compare to 100^o of the air pressurized actuator), the maximum generated force at that angle is the same one as the one generated using the air pressurized part. In addition, the hydraulic actuator demonstrated the highest generated force compare to all other designs: close to 0.4N, which is more than 2X higher than the one generated from the pneumatic (0.175N). A reason for that, is because the actuator withstood 3 bar of hydraulic pressure and compare to the 3rd design's maximum air pressure, is again more than 2X higher.

Overall, actuating the part with hydraulic pressure seems to respond better than with air pressure. A reason for that, might be the incompressibility of water. For the pneumatic actuator, for example, when the pressure was set to 1.2 bar it was slowly decreasing and finally settling at 1 bar. That is a result of the compressibility of air and it highly influence the outcome results.

D. SLS Printed Actuator

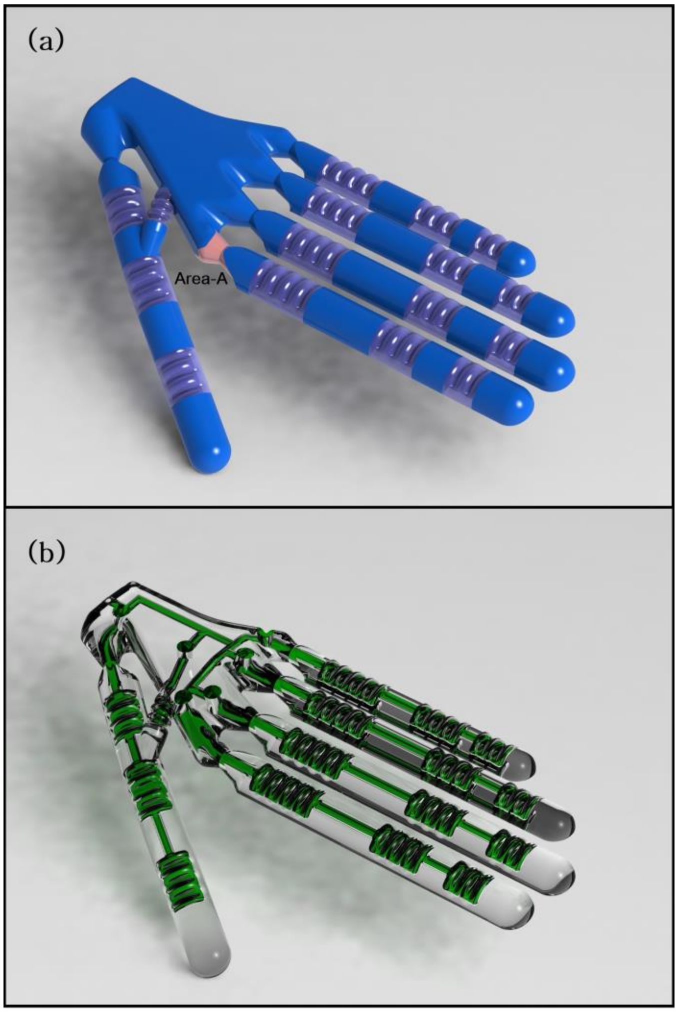

Fig. 21: a) Prototype design of a hand assistive exoskeleton device. Area-A demonstrates the thinner connection from the intercarpal to the finger, allowing some freedom for ad(b)duction of patient's finger and b) soft actuators (3rd design) as well as a fluidic circuit to control the device are embedded in the design. The fluidic circuit is design to accept plug-in on/off valves from: The Lee Company [59], one for each finger and two for the thumb.

The SLS printed actuator demonstrated extreme tolerance to high pressures. It can withstand more than 7 bar of pressure but the actuator didn't bend at all. The reason behind the immobility is the wall-thickness of the actuator. Contradictory to MJP technology, SLS prints with a single material, meaning that the stiffness of the material will be the same. Printing the same wall thickness to the entire part will result to the same stiffness to the actuator, thus the lack of motion. An easy fix to this problem could be a design with variable wall-thickness, thinner to reduce the stiffness and thicker to increase it. Due to the lack of time, no additional SLS printed parts have been prepared, but that would be very interesting for further research. That's because the elsto-plastic material, even with a wall thickness of 1.5mm, proved to handle high pressures without any signs of sallowness. Reducing the wall-thickness will make the actuator weaker, but it might still be able to handle much higher pressures than the MJP parts.

VII. 3D-Printed Hand Assisting Device

As an addition to this study and for motivation purposes for further studies on 3D-printed soft actuators, the feasibility of the development of a single-part 3D-printed hand exoskeleton device was investigated. Even though, according to the results, the actuators do not fill the functionality requirements to support such a device due to low generated force, a hand assisting device was designed and it's presented in fig. 21a. The actuators used in the design (transparent regions) are based on the 3rd actuator design without the reinforcement rings. The device was not printed or tested because according to the results from the actuator tests, is not able to fulfill the functional requirements. Nevertheless, after succeeding on the development of an actuator that can produce enough force, someone can adapt the new actuator design on the hand exoskeleton design, concluding to a product that is ready for test.

In fig. 21b, the embedded fluidic circuit is shown. For the control of the device, plug-in valves can be placed for each finger as it's shown, or one for two fingers for combined fingers movement. Miniature fluidic valves, small enough to fit to the design are commercially available (e.g. LHD Series Solenoid Valves from: The Lee Company [59]), and by using the approach of combined fingers motion, the number of valves needed are minimized, resulting to a cheaper device. For the pressurization of the circuit, a pump, or even a master cylinder with a ball screw and an electric motor attached can be used. The pump or the cylinder can be attached to the wrist for an easy fit, but if the weight is too much for the patient, he can chose to place it anywhere else (i.e. to the upper arm) and connect it to the device with flexible tubes.

The way that the device is designed, actuates 16 DOF, but due to the thin interconnection between the main part and the fingers (fig. 21a, area-A), it also allows some free adduction/abduction of the fingers. In addition, if the device is printed with MJP printer, the stiffness of area-A can be adjusted according to the patient's needs. For example if the patient

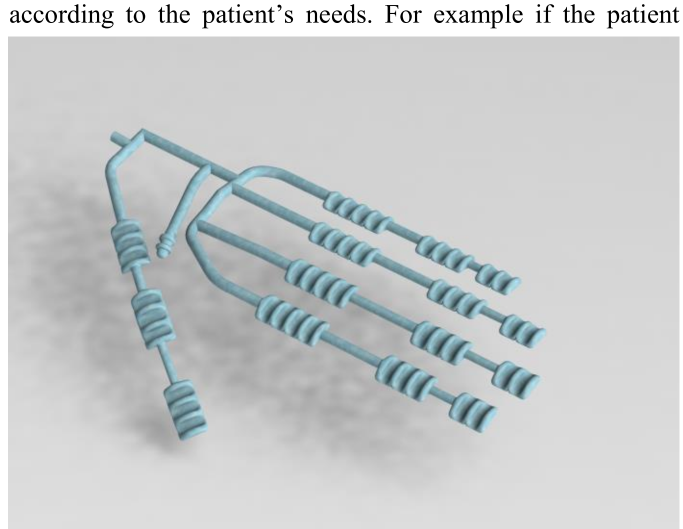

Fig. 22: Internal circuit and actuators' chambers result to a total volume of 28.05cm^3, which means that by using air, 0.034gr are added to the total weight of the device, and by using water, 28.05gr.

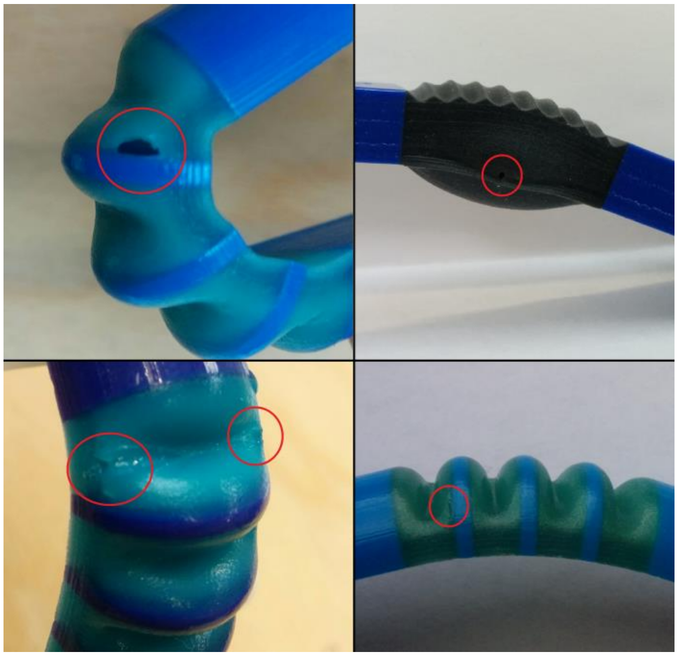

Fig. 23: Failure points of 4 different actuators (after testing). Even though four are presented, in all cases the failure point was located either on the side or in-between two chambers (on the top of the actuator).

needs more stability, area-A should be stiffer compare to the case that the patient needs more freedom.

Another benefit of the design, is that it allows an easy parameterization, leading to an easy adaptability on different patients. With simple measurements like the length and width of the patient's fingers and the width of the palm at several points, the device could be adjusted to the patient's hand.

IIX. Results

A conceptual design of an assistive exoskeleton device for DMD patients, has been is presented. The smart design includes the fluidic circuit and the actuators. Since the actuators that were used on the design have been tested, requirement check is possible.

Starting from the DOFs, as it was mentioned to the previous section, the design of the device includes 16 active and 5 passive resulting to a total of 21 out of 23 DOFs that a human hand has. It is important to mention that, from the 16 actuators not all of them can be activated separately. According to the position and number of control valves, all the actuators from one, two or four (index, middle, ring and small) fingers are activated at once. The thumb, has a separate control valve from the other fingers which controls all three actuators of the thumb.

Be able to, not only 3D-print soft actuators, but also monolithic devices that use multiple actuators, helps with weight and space management of the device. Even if the device has 16 actuators, no additional mechanical parts are needed to interconnect them to it, making the device one of the smallest (with a total volume estimated to be: 117.1cm^3) and most lightweight exoskeletons. Since the final exoskeleton is just a design, an estimation of its weight has been calculated, using SolidWorks. The design is so compact that no matter what kind

TABLE III

Results Compared With Requirements

Specification	Required	Result
DOFs	23 in total	16 active 5 passive
Weight	<500gr	Achieved (<150gr)
Space	Small and Elegant	Achieved
Safety	No harm to patient	Achieved
Functionality	Min 1Np.a.*	Failed
ROM	Functional: max 85^o	Achieved

*Newton per actuator

of plastic is used, it never overpasses 150gr. This estimation is: a) without the control valves that according to The Lee Company weigh 2.5gr each [59], b) without the working fluid (the volume of the internal fluidic circuit (fig. 22) has been estimated to be 28.05 cm^3 resulting to: 0.034gr of air or 28.05gr of water) and c) without the master cylinder or the pump (that can be placed elsewhere, e.g. the upper arm).

For the safety of the device, the actuators are designed such that, their weak points to be on their side. In combination with the low pressure activation at the time of failure, the actuators fail from the side (that the finger is safe). Fig. 23, demonstrates failure points of some of the tested actuators. At last, moving to the functionality and the ROM of the actuators, even though the maximum generated force was too small (50x smaller than the required), their ROM covers the required one. Table III summarizes the needed requirements (from Section III) and the outcome results of the study.

IX. Discussion and Conclusions

In this study, a proposal of a new type of an assisting exoskeleton device for DMD patients is investigated. Soft hydraulic actuators were designed to support the device. Even though the results revealed that there is a need for further research for such actuator, the technology to build one already exist, and a lot of researches already turned their focus on the exploitation of that technology.

Nevertheless, the outcome of this study demonstrated that the maximum generated force at 85^o is 0.023N that is 50x smaller than the one that is required. Among different actuator designs, the actuator with 3 reinforcement rings with the same wall thickness as the wall thickness of the device (3rd design, fig. 15a) printed with the soft material to be 70% stiff and actuated with pressurized water, demonstrated the best performance. In addition, the design was adjusted for SLS printing, and printed using an elasto-plastic material. It demonstrated higher tolerance to the pressure, since it was tested with a pressure up to 7 bar and didn't fail. On the other hand, that actuator didn't have any motion, due to a geometric condition that was discussed in Section VI. The conclusion is that the elasto-plastic material that was used, seems to be more promising, for succeeding in printing an actuator that fulfills the requirements for an assisting device. Except from the material, another factor that made the SLS printed part stronger than the MJP printed part is the cleaning procedure. As it was mentioned earlier, the cleaning procedure for MJP parts lasted several days and involved chemicals that were slowly dissolving not only the support material, but also the soft material. A dissolved

Fig. 24: Corrosion of the inner walls of the actuator's chamber, due to chemical cleaning procedure of the support material. The corrosion has weakened the soft material to a point that it failed without pressurizing it.

chamber due to the cleaning process is represented in fig. 24. On the contrary, despite some dimensional adjustments, cleaning process of SLS printed parts is much simpler and material friendly. Support material is powder, so it is removed from the chamber without damaging the part, just by blowing pressurized air inside.

Regardless the results of the actuators, the design of the exoskeleton device is still presented as an intellectual nourishment for future studies. The device has 16 active and 5 passive DOF and with a total volume of around 117.1 cm^3 could result to a lightweight device of less than 150gr (printed on any kind of plastic). In addition, the design allows easy adaptability to different patients and it is also cosmetically acceptable. Lastly, unfortunately in this study, the exoskeleton device hasn't been tested so the usage simplicity wasn't recorded, but in theory after 3D printing the device it should be ready to use.

X. Future Work

A monolithic 3D-printed hand assistive device might seem to be beneficial to the weight and space requirements, but there are a lot of missing steps to move from design to product. Further research is still needed for the development of a 3D-printed fluidic actuator that could support the device.

First step is to think on what technique is going to be used. Most of the current research is about using 3D-printing technique with the MJP technology. Support material was limiting the minimum scale of the inner structure and therefore the dimensions of the whole design. In addition, the chemical procedure that is required for its extraction (or cleaning process) damages the inner walls of the actuator (see fig. 24), resulting to unclear conclusions about this technique. An interesting step forward for using MJP technology will be to print the soft actuator using wax as support material (and therefore cleaning process will be low hit treatment), or water (as it was discussed in Section IV) resulting to a prefilled final product.

In addition, a small step for using SLS printing technology has been made. An advantage of using SLS instead of MJP technology is that the support material that is used is powder, making the cleaning process much easier and faster. Again, the support material is the main limiting factor for the scaling down the dimensions and a disadvantage is that multiple stiffness printing is not possible. Elasto-plastic materials that can be used for printing soft actuators exist, but since the stiffness doesn't change, the design has a major impact on the behavior of the actuator. The elasto-plastic material that was used in this study, demonstrated advanced resistance to internal pressures, reaching 7 bar without any signs of failure. On the contrary, due to bad design choices (wall-thickness and/or internal shape of the actuator), there was almost no movement. Figuring out the correlation of the design with the behavior of the actuator and adjusting actuator chamber's wall thickness could be an innovating step in future studies.

Finally, moving to a totally different technique, might also be a smart choice for future research. Using molds or different chamber shapes (i.e. balloon shape chambers) demonstrated good results in previous studies (see Section IV). Even though molds were not used in this study, using this technique to adapt multiple stiffness in a single part could be beneficial from the material point of view. Many more choices are available than 3D-printable materials, also for support materials, making wax one of the most commonly used.

Acknowledgment

I would like to thank professor Dr. ir. D.H. Plettenburg, PhD student Ronald Bos and researcher MSc Scharff, R.B.N. for their guidance and feedback on this study. In addition, special thanks to George Kiliaris, Irineos Loizou and Christos Kyprianou for their additional inputs, advises and corrections on this report. Lastly, special thanks to TU Delft professor J.A.S. van Driel, from the faculty of 3ME, which helped with the development of a NI LabVIEW program responsible for the data compilation.

References

[1] Mayo Clinic. (2018). *Muscular dystrophy - Symptoms and causes*. [online] Available at: https://www.mayoclinic.org/diseases-conditions/muscular-dystrophy/symptoms-causes/syc-20375388 [Accessed 3 Dec. 2017].

[2] Monckton, G., Hoskin, V. and Warren, S., 1982. Prevalence and incidence of muscular dystrophy in Alberta, Canada. *Clinical genetics*, *21*(1), pp.19-24.

[3] Disabled World. 2015. *Muscular Dystrophy: Facts, News & Information*. [ONLINE] Available at: https://www.disabled-world.com/disability/types/mobility/md/. [Accessed 27 February 2017].

[4] Koenig, M., Hoffman, E.P., Bertelson, C.J., Monaco, A.P., Feener, C. and Kunkel, L.M., 1987. Complete cloning of the Duchenne muscular dystrophy (DMD) cDNA and preliminary genomic organization of the DMD gene in normal and affected individuals. *Cell*, *50*(3), pp.509-517.

[5] Kunkel, L.M., 1986. Analysis of deletions in DNA from patients with Becker and Duchenne muscular dystrophy. *Nature*, *322*(6074), pp.73-77.

[6] Jones, H.R., Darryl, C. and Darras, B.T. eds., 2003. *Neuromuscular disorders of infancy, childhood, and adolescence: a clinician's approach*. Butterworth-Heinemann.

[7] Perloff, J.K., 1984. Cardiac rhythm and conduction in Duchenne's muscular dystrophy: a prospective study of 20 patients. *Journal of the American College of Cardiology*, *3*(5), pp.1263-1268.

[8] Chenard, A.A., Becane, H.M., Tertrain, F., De Kermadec, J.M. and Weiss, Y.A., 1993. Ventricular arrhythmia in Duchenne muscular dystrophy: prevalence, significance and prognosis. *Neuromuscular Disorders*, *3*(3), pp.201-206.

[9] Sussman, M., 2002. Duchenne muscular dystrophy. *Journal of the American Academy of Orthopaedic Surgeons*, *10*(2), pp.138-151.

[10] Emery, A.E., Muntoni, F. and Quinlivan, R.C., 2015. *Duchenne muscular dystrophy*. OUP Oxford.

[11] Muscular Dystrophy Association. 2015. Duchenne Muscular Dystrophy (DMD). [ONLINE] Available at: https://www.mda.org/disease/duchenne-muscular-dystrophy. [Accessed 26 January 2017].

[12] Yoshioka, M., Okuno, T., Honda, Y. and Nakano, Y., 1980. Central nervous system involvement in progressive muscular dystrophy. Archives of disease in childhood, 55(8), pp.589-594.

[13] Huber, J.E., Fleck, N.A. and Ashby, M.F., 1997, October. The selection of mechanical actuators based on performance indices. In *Proceedings of the Royal Society of London A: Mathematical, Physical and Engineering Sciences* (Vol. 453, No. 1965, pp. 2185-2205). The Royal Society.

[14] Brown, M., Tsagarakis, N. and Caldwell, D.G., 2003. Exoskeletons for human force augmentation. Industrial Robot: An International Journal, 30(6), pp.592-602.

[15] MacCurdy, R., Katzschmann, R., Kim, Y. and Rus, D., 2016, May. Printable hydraulics: a method for fabricating robots by 3D co-printing solids and liquids. In *Robotics and Automation (ICRA), 2016 IEEE International Conference on* (pp. 3878-3885). IEEE.

[16] Bergamasco, M., Frisoli, A. and Avizzano, C.A., 2007. Exoskeletons as man-machine interface systems for teleoperation and interaction in virtual environments. In Advances in Telerobotics (pp. 61-76). Springer Berlin Heidelberg.

[17] Favetto, A., Chen, F.C., Ambrosio, E.P., Manfredi, D. and Calafiore, G.C., 2010, December. Towards a hand exoskeleton for a smart EVA glove. In Robotics and Biomimetics (ROBIO), 2010 IEEE International Conference on (pp. 1293-1298). IEEE.

[18] Heo, P., Gu, G.M., Lee, S.J., Rhee, K. and Kim, J., 2012. Current hand exoskeleton technologies for rehabilitation and assistive engineering. International Journal of Precision Engineering and Manufacturing, 13(5), pp.807-824.

[19] Arata, J., Ohmoto, K., Gassert, R., Lambercy, O., Fujimoto, H. and Wada, I., 2013, May. A new hand exoskeleton device for rehabilitation using a three-layered sliding spring mechanism. In Robotics and Automation (ICRA), 2013 IEEE International Conference on (pp. 3902-3907). IEEE.

[20] C.J. Nycz, T. Butzer, O. Lambercy, J. Arata, G.S. Fisher and R. Gassert, "Design and Characterization of a Lightweight and Fully Portable Remote Actuation System for Use with a Hand Exoskeleton," IEEE Robotics and Automation Letters, 2016, pp. 976983.

[21] Aubin, P.M., Sallum, H., Walsh, C., Stirling, L. and Correia, A., 2013, June. A pediatric robotic thumb exoskeleton for at-home rehabilitation: the isolated orthosis for thumb actuation (IOTA). In Rehabilitation Robotics (ICORR), 2013 IEEE International Conference on (pp. 1-6). IEEE.

[22] Kooren, P.N., Lobo-Prat, J., Keemink, A.Q., Janssen, M.M., Stienen, A.H., de Groot, I.J., Paalman, M.I., Verdaasdonk, R. and Koopman, B.F., 2016, June. Design and control of the Active A-Gear: A wearable 5 DOF arm exoskeleton for adults with Duchenne muscular dystrophy. In *Biomedical Robotics and Biomechatronics (BioRob), 2016 6th IEEE International Conference on* (pp. 637-642). IEEE.

[23] Polygerinos, P., Galloway, K.C., Savage, E., Herman, M., O'Donnell, K. and Walsh, C.J., 2015, May. Soft robotic glove for hand rehabilitation and task specific training. In Robotics and Automation (ICRA), 2015 IEEE International Conference on (pp. 2913-2919). IEEE.

[24] Polygerinos, P., Wang, Z., Galloway, K.C., Wood, R.J. and Walsh, C.J., 2015. Soft robotic glove for combined assistance and at-home rehabilitation. Robotics and Autonomous Systems, 73, pp.135-143.

[25] Wege, A. and Hommel, G., 2005, August. Development and control of a hand exoskeleton for rehabilitation of hand injuries. In *Intelligent Robots and Systems, 2005. (IROS 2005). 2005 IEEE/RSJ International Conference on* (pp. 3046-3051). IEEE.

[26] Wege, A. and Zimmermann, A., 2007, December. Electromyography sensor based control for a hand exoskeleton. In *Robotics and Biomimetics, 2007. ROBIO 2007. IEEE International Conference on* (pp. 1470-1475). IEEE.

[27] Molenbroek, J.F., 2004. DINED, Anthropometric database. *Delft University of Technology*.

[28] Worsnopp, T.T., Peshkin, M.A., Colgate, J.E. and Kamper, D.G., 2007, June. An actuated finger exoskeleton for hand rehabilitation following stroke. In Rehabilitation Robotics, 2007. ICORR 2007. IEEE 10th International Conference on (pp. 896-901). IEEE.

[29] Nakagawara, S., Kajimoto, H., Kawakami, N., Tachi, S. and Kawabuchi, I., 2005, April. An encounter-type multi-fingered master hand using circuitous joints. In Robotics and Automation, 2005. ICRA 2005. Proceedings of the 2005 IEEE International Conference on (pp. 2667-2672). IEEE.

[30] Wang, J., Li, J., Zhang, Y. and Wang, S., 2009, September. Design of an exoskeleton for index finger rehabilitation. In Engineering in Medicine and Biology Society, 2009. EMBC 2009. Annual International Conference of the IEEE (pp. 5957-5960). IEEE.

[31] Matheus, K. and Dollar, A.M., 2010, October. Benchmarking grasping and manipulation: Properties of the objects of daily living. In Intelligent Robots and Systems (IROS), 2010 IEEE/RSJ International Conference on (pp. 5020-5027). IEEE.

[32] Smaby, N., Johanson, M.E., Baker, B. and Kenney, D.E., 2004. Identification of key pinch forces required to complete functional tasks. Journal of rehabilitation research and development, 41(2), p.215.

[33] Lee, Y. and Ryu, D., 2008, August. Wearable haptic glove using micro hydraulic system for control of construction robot system with VR environment. In Multisensor Fusion and Integration for Intelligent Systems, 2008. MFI 2008. IEEE International Conference on (pp. 638-643). IEEE.

[34] Schulz, A., Pylatiuk, C., Kargov, A., Oberle, R. and Bretthauer, G., 2004, September. Progress in the development of anthropomorphic fluidic hands and their applications. In Mechatronics & Robotics (pp. 936-941).

[35] Schulz, S., Pylatiuk, C. and Bretthauer, G., 2001. A new ultralight anthropomorphic hand. In Robotics and Automation, 2001. Proceedings 2001 ICRA. IEEE International Conference on (Vol. 3, pp. 2437-2441). IEEE.

[36] Smit, G., Plettenburg, D.H. and van der Helm, F.C., 2015. The lightweight Delft Cylinder Hand: first multi-articulating hand

that meets the basic user requirements. IEEE Transactions on Neural Systems and Rehabilitation Engineering, 23(3), pp.431-440.

[37] Heather, A.J. and Smith, T.A., 1960. Helping hand, a hydraulically operated mechanical hand. Orthopedic and Prosthetic Appliance Journal, p.14.

[38] Broome, D.R., Davies, B.L. and Lord, M., 1974. A total hydraulically powered prosthetic arm system. Engineering in Medicine, 3(2), pp.8-14.

[39] Kargov, A., Werner, T., Pylatiuk, C. and Schulz, S., 2008. Development of a miniaturised hydraulic actuation system for artificial hands. Sensors and Actuators A: Physical, 141(2), pp.548-557.

[40] Bouzit, M., Burdea, G., Popescu, G. and Boian, R., 2002. The Rutgers Master II-new design force-feedback glove. IEEE/ASME Transactions on mechatronics, 7(2), pp.256-263.

[41] Tadano, K., Akai, M., Kadota, K. and Kawashima, K., 2010, May. Development of grip amplified glove using bi-articular mechanism with pneumatic artificial rubber muscle. In Robotics and Automation (ICRA), 2010 IEEE International Conference on (pp. 2363-2368). IEEE.

[42] Kiminori, T.O.Y.A., Miyagawa, T. and Kubota, Y., 2011. Power-assist glove operated by predicting the grasping mode. Journal of System Design and Dynamics, 5(1), pp.94-108.

[43] Plettenburg, D.H., 2002, 'A sizzling hand prosthesis. On the design and development of a pneumatically powered hand prosthesis for children', PhD thesis, Delft University of Technology, The Netherlands.

[44] Hume, M.C., Gellman, H., McKellop, H. and Brumfield, R.H., 1990. Functional range of motion of the joints of the hand. *The Journal of hand surgery*, *15*(2), pp.240-243.

[45] Yap, H.K., Lim, J.H., Nasrallah, F., Goh, J.C. and Yeow, R.C., 2015, May. A soft exoskeleton for hand assistive and rehabilitation application using pneumatic actuators with variable stiffness. In *Robotics and Automation (ICRA), 2015 IEEE International Conference on* (pp. 4967-4972). IEEE.

[46] Yap, H.K., Goh, J.C.H. and Yeow, R.C.H., 2015. Design and characterization of soft actuator for hand rehabilitation application. In *6th European Conference of the International Federation for Medical and Biological Engineering* (pp. 367-370). Springer, Cham.

[47] Yap, H.K., Lim, J.H., Nasrallah, F., Cho Hong Goh, J. and Yeow, C.H., 2016. Characterisation and evaluation of soft elastomeric actuators for hand assistive and rehabilitation applications. *Journal of medical engineering & technology*, *40*(4), pp.199-209.

[48] Low, J.H., Ang, M.H. and Yeow, C.H., 2015, August. Customizable soft pneumatic finger actuators for hand orthotic and prosthetic applications. In *Rehabilitation Robotics (ICORR), 2015 IEEE International Conference on* (pp. 380-385). IEEE.

[49] Konishi, S., Nokata, M., Jeong, O.C., Kusuda, S., Sakakibara, T., Kuwayama, M. and Tsutsumi, H., 2006, May. Pneumatic micro hand and miniaturized parallel link robot for micro manipulation robot system. In *Robotics and Automation, 2006. ICRA 2006. Proceedings 2006 IEEE International Conference on* (pp. 1036-1041). IEEE.

[50] Ilievski, F., Mazzeo, A.D., Shepherd, R.F., Chen, X. and Whitesides, G.M., 2011. Soft robotics for chemists. *Angewandte Chemie*, *123*(8), pp.1930-1935.

[51] Zhao, H., Li, Y., Elsamadisi, A. and Shepherd, R., 2015. Scalable manufacturing of high force wearable soft actuators. *Extreme Mechanics Letters*, *3*, pp.89-104.

[52] Scharff, R.B., Doubrovski, E.L., Poelman, W.A., Jonker, P.P., Wang, C.C. and Geraedts, J.M., 2017. Towards Behavior Design of a 3D-Printed Soft Robotic Hand. In *Soft Robotics: Trends, Applications and Challenges* (pp. 23-29). Springer International Publishing.

[53] Rus, D. and Tolley, M.T., 2015. Design, fabrication and control of soft robots. *Nature*, *521*(7553), pp.467-475.

[54] YouTube. (2018). *Powering the New HP Jet Fusion 3D Printers | Jet Fusion 3D Printing | HP*. [online] Available at: https://www.youtube.com/watch?v=VXntl3ff5tc [Accessed 4 Dec. 2017].

[55] YouTube. (2018). *3D Systems MultiJet Printing (MultiJet Modeling) process*. [online] Available at: https://www.youtube.com/watch?v=apm5Gn2s_-M [Accessed 5 Dec. 2017].

[56] 3D Systems. (2018). *What is MJP (MultiJet Printing)? | 3D Systems*. [online] Available at: https://www.3dsystems.com/resources/information-guides/multi-jet-printing/mjp [Accessed 5 Dec. 2017].

[57] 3D Printing from scratch. (2018). *Types of 3D printers or 3D printing technologies overview | 3D Printing from scratch*. [online] Available at: http://3dprintingfromscratch.com/common/types-of-3d-printers-or-3d-printing-technologies-overview/#fdm [Accessed 7 Dec. 2017].

[58] Shapeways.com. (2018). *Elasto Plastic 3D Printing Rubber Material Information - Shapeways*. [online] Available at: https://www.shapeways.com/materials/elasto-plastic [Accessed 6 Dec. 2017].

[59] Theleeco.com. (2018). *LHD Series Solenoid Valves - 2-Port Plug-In: Conventional and Lo-Lohm Models*. [online] Available at: http://www.theleeco.com/electro-fluidic-systems/solenoid-valves/lhd/2-port-plug-in-solenoid-valves.cfm [Accessed 4 Dec. 2017].

[60] ORD Solutions Inc. (2018). *RoVa3D 5 Extruder 3D Printer Package - SOLD OUT*. [online] Available at: https://www.ordsolutions.com/rova3d-5-extruder-3d-printer-package/ [Accessed 5 Dec. 2017].

[61] Tiwari, R., Meller, M.A., Wajcs, K.B., Moses, C., Reveles, I. and Garcia, E., 2012. Hydraulic artificial muscles. Journal of Intelligent Material Systems and Structures, 23(3), pp.301-312.

[62] Cool, J.C. and Van Hooreweder, G.J., 1971. Hand prosthesis with adaptive internally powered fingers. Medical and Biological Engineering and Computing, 9(1), pp.33-36.

[63] Menon, C. and Lira, C., 2006. Active articulation for future space applications inspired by the hydraulic system of spiders. Bioinspiration & biomimetics, 1(2), p.52.

[64] Meller, M. and Garcia, E., 2013, April. Bioinspired hydraulic control systems. In SPIE Smart Structures and Materials+ Nondestructive Evaluation and Health Monitoring (pp. 868603-868603). International Society for Optics and Photonics.

[65] Xia, J. and Durfee, W.K., 2013. Analysis of small-scale hydraulic actuation systems. Journal of mechanical design, 135(9), p.091001.

[66] Plattenburg, D.H., 2005, July. Pneumatic actuators: a comparison of energy-to-mass ratio's. In Rehabilitation Robotics, 2005. ICORR 2005. 9th International Conference on (pp. 545-549). IEEE.

[67] Peirs, J., Reynaerts, D. and Van Brussel, H., 2000. Design of miniature parallel manipulators for integration in a self-propelling endoscope. Sensors and Actuators A: Physical, 85(1), pp.409-417.

[68] Love, L.J., Lind, R.F. and Jansen, J.F., 2009, October. Mesofluidic actuation for articulated finger and hand prosthetics. In Intelligent Robots and Systems, 2009. IROS 2009. IEEE/RSJ International Conference on (pp. 2586-2591). IEEE.

[69] Li, B., Chen, Q., Lee, D.G., Woolman, J. and Carman, G.P., 2005. Development of large flow rate, robust, passive micro

check valves for compact piezoelectrically actuated pumps. Sensors and Actuators A: Physical, 117(2), pp.325-330.
[70] Li, B. and Chen, Q., 2005. Design and fabrication of in situ UV-LIGA assembled robust nickel micro check valves for compact hydraulic actuators. Journal of Micromechanics and Microengineering, 15(10), p.1864.
[71] Roberts, D.C., Hagood, N.W., Su, Y.H., Li, H. and Carretero, J.A., 2000, June. Design of a piezoelectrically driven hydraulic amplification microvalve for high-pressure high-frequency applications. In SPIE's 7th Annual International Symposium on Smart Structures and Materials (pp. 616-628). International Society for Optics and Photonics.
[72] Roberts, D.C., Yaglioglu, O., Carretero, J., Su, Y.H., Saggere, L. and Hagood, N.W., 2001, August. Modeling, design, and simulation of a piezoelectrically driven microvalve for high pressure, high frequency applications. In Proc. of SPIE (Vol. 4327, pp. 4-8).
[73] Roberts, D.C., Li, H., Steyn, J.L., Yaglioglu, O., Spearing, S.M., Schmidt, M.A. and Hagood, N.W., 2003. A piezoelectric microvalve for compact high-frequency, high-differential pressure hydraulic micropumping systems. Journal of Microelectromechanical Systems, 12(1), pp.81-92.
[74] Lind, R.F., Lind Randall F, 2012. Mesofluidic shape memory alloy valve. U.S. Patent Application 13/020,633.
[75] Love, L.J., Jansen, J.F. and Lind, R.F., UT-Battelle. LLC, 2013. Mesofluidic digital valve. U.S. Patent Application 14/022,859.
[76] Weisener, T., Voegele, G., Widmann, M., Bark, C., Schraft, R.D., Bertholds, A. and Braunschweiler, A., 1996, September. Development and fabrication of a rotary micropump and its industrial and medical applications. In Micromachining and Microfabrication'96 (pp. 218-225). International Society for Optics and Photonics.
[77] Rodriguez, D., Massachusetts Institute of Technology, 1998. Power-assisted upper extremity orthosis. U.S. Patent 5,800,561.
[78] DiCicco, M., Lucas, L. and Matsuoka, Y., 2004, April. Comparison of control strategies for an EMG controlled orthotic exoskeleton for the hand. In Robotics and Automation, 2004. Proceedings. ICRA'04. 2004 IEEE International Conference on (Vol. 2, pp. 1622-1627). IEEE.
[79] Allington, J., Spencer, S.J., Klein, J., Buell, M., Reinkensmeyer, D.J. and Bobrow, J., 2011, August. Supinator extender (SUE): a pneumatically actuated robot for forearm/wrist rehabilitation after stroke. In Engineering in Medicine and Biology Society, EMBC, 2011 Annual International Conference of the IEEE (pp. 1579-1582). IEEE.
[80] Pylatiuk, C., Kargov, A., Gaiser, I., Werner, T., Schulz, S. and Bretthauer, G., 2009, June. Design of a flexible fluidic actuation system for a hybrid elbow orthosis. In Rehabilitation Robotics, 2009. ICORR 2009. IEEE International Conference on (pp. 167-171). IEEE.
[81] Kline, T., Kamper, D. and Schmit, B., 2005, June. Control system for pneumatically controlled glove to assist in grasp activities. In Rehabilitation Robotics, 2005. ICORR 2005. 9th International Conference on (pp. 78-81). IEEE.
[82] Xing, K., Xu, Q., He, J., Wang, Y., Liu, Z. and Huang, X., 2008, October. A wearable device for repetitive hand therapy. In Biomedical Robotics and Biomechatronics, 2008. BioRob 2008. 2nd IEEE RAS & EMBS International Conference on (pp. 919-923). IEEE.
[83] Wu, J., Huang, J., Wang, Y. and Xing, K., 2010, November. A wearable rehabilitation robotic hand driven by PM-TS actuators. In International Conference on Intelligent Robotics and Applications (pp. 440-450). Springer Berlin Heidelberg.
[84] Chakraborty, I., Tang, W.C., Bame, D.P. and Tang, T.K., 2000. MEMS micro-valve for space applications. Sensors and Actuators A: Physical, 83(1), pp.188-193.
[85] Rogge, T., Rummler, Z. and Schomburg, W.K., 2004. Polymer micro valve with a hydraulic piezo-drive fabricated by the AMANDA process. Sensors and Actuators A: Physical, 110(1), pp.206-212.
[86] Yang, B. and Lin, Q., 2007. Planar micro-check valves exploiting large polymer compliance. Sensors and Actuators A: Physical, 134(1), pp.186-193.
[87] Klasson, B.L., 1967. Development on externally powered artificial arms at NBI. In Proceedings of the International Symposium on External Control of Human Extermities, August 29 – September 2, 1966, Dubrovnik, Yugoslavia (pp. 157-173).
[88] Pistecky, P.V., 1971, ‘Optimization of an electrically operated proportional valve’, MSc thesis, Department of Mechanical Engineering, Delft University of Technology, The Netherlands.
[89] Cool, J.C. and Pistecky, P.V., 1971. Miniature electrically operated proportional valve. Proceedings on Human Locomotor Engineering, p.27.
[90] Hekman, E.E.G., 1987, ‘Myo-pneumatic prosthesis for children’, MSc thesis, Department of Mechanical Engineering, Delft University of Technology, The Netherlands.
[91] Esashi, M., 1990. Integrated micro flow control systems. Sensors and Actuators A: Physical, 21(1-3), pp.161-167.
[92] Gongora-Rubio, M., Sola-Laguna, L., Smith, M.A. and Santiago-Aviles, J.J., 1999, August. Mesoscale electromagnetically actuated normally closed valve realized on LTCC tapes. In Symposium on Micromachining and Microfabrication (pp. 230-239). International Society for Optics and Photonics.
[93] Yoo, J.H. and Wereley, N.M., 2002. Design of a high-efficiency magnetorheological valve. Journal of Intelligent Material Systems and Structures, 13(10), pp.679-685.
[94] Tu, H.C., Rannow, M.B., Wang, M., Li, P.Y., Chase, T.R. and Van de Ven, J.D., 2012. Design, modeling, and validation of a high-speed rotary pulse-width-modulation on/off hydraulic valve. Journal of dynamic systems, measurement, and control, 134(6), p.061002.
[95] Bryant, M., Fitzgerald, J., Miller, S., Saltzman, J., Kim, S., Lin, Y. and Garcia, E., 2014, March. Climbing robot actuated by meso-hydraulic artificial muscles. In SPIE Smart Structures and Materials+ Nondestructive Evaluation and Health Monitoring (pp. 90570H-90570H). International Society for Optics and Photonics.
[96] Kamper, K.P., Dopper, J., Ehrfeld, W. and Oberbeck, S., 1998, January. A self-filling low-cost membrane micropump. In Micro Electro Mechanical Systems, 1998. MEMS 98. Proceedings., The Eleventh Annual International Workshop on (pp. 432-437). IEEE.
[97] Park, J.H., Yoshida, K. and Yokota, S., 1997. A piezoelectric micropump using resonance drive: proposal of resonance drive and basic experiments on pump characteristics. Fluid Power Systems and Technology: Corrected Paper ASME 1997.
[98] Park, J.H., Yoshida, K. and Yokota, S., 1999. Resonantly driven piezoelectric micropump: Fabrication of a micropump having high power density. Mechatronics, 9(7), pp.687-702.
[99] Zeng, S., Chen, C.H., Mikkelsen, J.C. and Santiago, J.G., 2001. Fabrication and characterization of electroosmotic micropumps. Sensors and Actuators B: Chemical, 79(2), pp.107-114.
[100] Paul, P.H., Arnold, D.W. and Rakestraw, D.J., 1998. Electrokinetic generation of high pressures using porous microstructures. In Micro Total Analysis Systems’ 98 (pp. 49-52). Springer Netherlands.
[101] Paul, P.H., Rakestraw, D.J., Arnold, D.W., Hencken, K.R., Schoeniger, J.S. and Neyer, D.W., Sandia Corporation, 2001. Electrokinetic high pressure hydraulic system. U.S. Patent 6,277,257.

[102] Li, H.Q., Roberts, D.C., Steyn, J.L., Turner, K.T., Carretero, J.A., Yaglioglu, O., Su, Y.H., Saggere, L., Hagood, N.W., Spearing, S.M. and Schmidt, M.A., 2000, June. A high frequency high flow rate piezoelectrically driven MEMS micropump. In 2000 Solid-State Sensor and Actuator Workshop (pp. 69-72).
[103] Doll, A.F., Wischke, M., Geipel, A., Goldschmidtboeing, F., Ruthmann, O., Hopt, U.T., Schrag, H.J. and Woias, P., 2007. A novel artificial sphincter prosthesis driven by a four-membrane silicon micropump. Sensors and Actuators A: Physical, 139(1), pp.203-209.
[104] Kim, H.T., Park, J.W. and Kim, H., 2011, June. All-electric peristaltic vacuum pump utilizing electromagnetic and hydraulic actuation with a highly flexible latex membrane. In Solid-State Sensors, Actuators and Microsystems Conference (TRANSDUCERS), 2011 16th International (pp. 2454-2457). IEEE.
[105] Son, J., Kim, H. and Kim, H., 2013, January. Pneumatic-less high-speed vacuum meso-pump driven by programmable hydraulics. In Micro Electro Mechanical Systems (MEMS), 2013 IEEE 26th International Conference on (pp. 584-587). IEEE.
[106] Al-Halhouli, A.T., Rawashdeh, N.A., Sanna, M., Büttgenbach, S. and Dietzel, A., 2015, November. Development of a novel electromagnetic double action meso-scale pump. In Research and Education in Mechatronics (REM), 2015 16th International Conference on (pp. 250-254). IEEE.
[107] Noritsugu, T., Yamamoto, H., Sasakil, D. and Takaiwa, M., 2004, August. Wearable power assist device for hand grasping using pneumatic artificial rubber muscle. In SICE 2004 Annual Conference (Vol. 1, pp. 420-425). IEEE.
[108] Sasaki, D., Noritsugu, T. and Takaiwa, M., 2005, April. Development of active support splint driven by pneumatic soft actuator (ASSIST). In Robotics and Automation, 2005. ICRA 2005. Proceedings of the 2005 IEEE International Conference on (pp. 520-525). IEEE.
[109] Garcia-Bonito, J., Brennan, M.J., Elliott, S.J., David, A. and Pinnington, R.J., 1998. A novel high-displacement piezoelectric actuator for active vibration control. Smart materials and structures, 7(1), p.31.

APPENDIX I: POWER DENSITY RATIO

Power density ratio is a useful measurement for choosing the correct technology for the actuation of the device. For the calculation of the power density ratio for the needed actuators, some of the requirements have been combined. In addition, since we don't have all the needed information, a lot of assumptions had to be made. Nevertheless, those are logical assumptions, so even if the exact ratio is not extracted, the calculations should not be far from true.

Assuming a needed force of 8 N (fingertip force) and an activation frequency of 5 Hz the power can be calculated. Using the functional ROM of the fingers of total arc of 131° (or 2.29 rad), the velocity can be calculated as follows:

$$U = \frac{x}{T} = ROM * r * f = 2.29 * 75 * 10^{-3} * 5 = 0.86\frac{m}{s} \quad (1)$$

with: T = Period
x = Distance
ROM = range of motion
r = radius: length of the finger (index finger for this case)
f = Frequency

Knowing the velocity the power can be calculated as:

$$P = F * U = 8 * 0.86 = 6.86\,W \quad (2)$$

with: F = fingertip force

In addition, by having the anthropometric data of the hand for the target group (middle finger length of 64 mm and a diameter of 10 mm) the volume of the actuator can be calculated as well. Assuming that one actuator will be used per finger, and that it should have less volume than the proximal phalanx of the finger the volume of the actuator can be calculated as (the proximal phalanx is assumed that concerns half of the finger's length):

$$V = \pi r^2 H = \pi\left(\frac{10}{2}\right)^2 32 = 2513\,mm^3 \quad (3)$$

with: H = length of the proximal phalanx
r = radius of the finger

Using that volume (2.51 × 10-6 m^3) and the needed power that was calculated in equation 2, an indication the power density ratio that is needed, can be calculated as:

$$n_{volume} = \frac{P}{V} = \frac{6.86}{2.51 * 10^{-6}} = 2.73 * 10^6\frac{W}{m^3} \quad (4)$$

That number indicates that actuators with less power density ration than that, cannot be miniaturized to the needed size and still be able to produce enough power. Power density ratios that correspond to fluidic actuators, some of the highest ratios between other technologies, overcome this number; for pneumatic actuators: 5 × 106 Wm^{-3} and for hydraulic actuators: 5 × 108 Wm^{-3}. That leads this study to the use of fluidic technology for the development of the hand exoskeleton.

APPENDIX II: 3D-PRINTING TECHNOLOGIES

For the purpose of this study some of the most popular 3D-printing technologies are analyzed. Due to the requirements, miniaturization is necessary, meaning that designing complexity and detailing increase. Different printing techniques for different purposes have been developed over the years and each one can result to different product resolution or complexity. Understanding their differences and how the most popular of those technologies work, it is necessary to decide on which 3D-printing technology is more suitable for the development of the hand exoskeleton.

Starting from the oldest developed 3D-printing method, StereoLithograph Apparatus or SLA works by solidifying liquid plastic. The main platform is submerged into liquid photopolymer resin, while an ultraviolet (UV) laser trace a pattern on that resign, which becomes a layer of the printed part. Exposure to UV laser solidifies the layer and bonds it to the previous one. When printing is done, the part is washed with a solvent (for the cleaning of the support material) and placed in a UV oven. This technology does not allow a combination of different materials and also, a support structure is needed, limiting designer's creativity. In addition, for the purpose of this study is worth mentioning that even though SLA printing

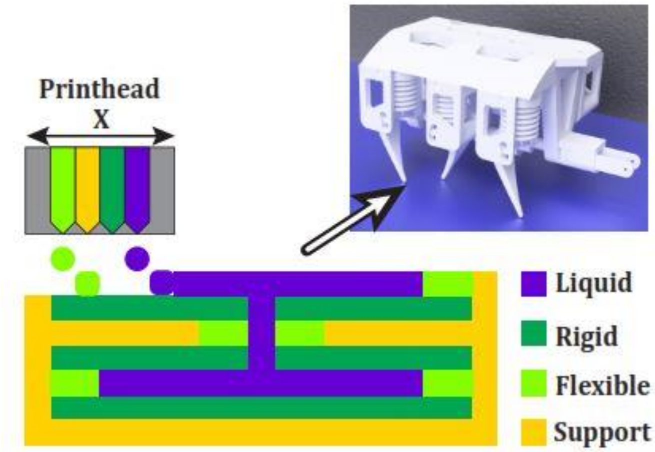

Fig. 25: A 3D printer simultaneously deposits solid and liquid regions within a printed assembly. Supporting layers are provided via removable support material or liquid. As an example, a hexapod robot can be printed in one step, requiring only a single DC motor. The motor pumps fluid through the robot's body, causing the legs to move by MacCurdy [15].

is relatively faster than other printing techniques, it is mostly being used for prototyping and only rarely for printing the final product [57].

On the other hand, Fused Deposition Modeling (FDM) printing is one of the most commonly used technology in product development. It uses a thermoplastic filament, which heats and extrudes it with a precise thickness with the help of an extrusion nozzle. By moving the nozzle in the X and Y axis and the main platform to the Z axis, it builds the part layer by layer, from the bottom up. Same as SLA printing, this technology also prints a support structure for the part, but in this case multiple materials can be used. FDM printers with multiple nozzles have been created [60], allowing to the designer to print with multiple thermoplastics or colors. Most commonly used thermoplastics are ABS (acrylonitrile butadiene styrene) and PC (polycarbonate). FDM technology result to anisotropic, but excellent mechanical properties, as well as thermal and chemical properties. In addition, support material can be water-soluble wax, giving more flexibility to the design [57].

Multi-Jet Printing (MJP) technology is one of the latest technologies developed. MJP works as a combination of the two former stated technologies. In this case, liquid plastic droplets are placed through the nozzle to create the layer and UV light is used to solidify it. By using liquid plastic the mixing of two materials is possible, allowing to the designer to print a part that can have different mechanical properties at different areas of the same part. Also, even though MJP technology, same as the previews two, uses support structure, the "liquid print" technique opens the opportunity to use a variety of support materiasl. An example is the recent study of MacCurdy [15] that alters an MJP 3D printer, to print water as an additional support material for inner structures (fig. 25). The resulting products have precision up to microns, better mechanical quality and are less anisotropic than FDM printed parts. A huge disadvantage is the cost of the printers that is unaffordable for even small companies [54-56].

The last technology that will be analyzed for the purpose of this study is Selective Laser Sintering (SLS). Unlike the other printing techniques, SLS uses powder material to print. Laser scans the shape of the layer onto the powder, causing the powder to melt together and bond with previous layers. One of the benefits of this technology is the variety of material that can be used; variety of plastics, ceramics, glass or even some metals like aluminum, steel or silver. In addition, with SLS printing, no support material is needed since the powder itself is used to support the structure. This is not entirely true, because for an inner structure, exit points must be designed such as the powder could be blown out after the process is finished. Even so, the designer has much more flexibility to 3D-print inner structures using this technology. On the other hand, the printers can be expensive but still cheaper than MJP printers, making this technology more suitable for manufacturing processes [57].

APPENDIX III: SUMMARY OF LITERATURE REVIEW ON MINIATURIZED HYDRAULIC COMPONENTS FOR A HAND EXOSKELETON

In this Appendix, a summary of a previews literature review on "Miniature Fluidic Components for a Hand Exoskeleton" (written by the same author), is presented. Table IV, V and VI summarize the basic information about fluidic valves, pumps and actuators that where researched and developed in previous studies. Due to the fact that some studies are missing necessary information, some of the specifications for specific components are filled with "N.M". (Not Mentioned). Dash means that the corresponding specification does not apply for that specific component.

According to Schylz's [35] and Kargov's [39] study, it is proven that a fully equipped hydraulic system can be designed in a scale to fit in a prosthetic, resulting to a fully functional device. Exoskeletons though, have less available space, and by using the same components (as one of those studies), could result to a bulkier and heavier exoskeleton than preferred. Other studies that developed a hand exoskeleton device, usually take advantage of the fact that hydraulics or pneumatics can be connected with flexible tubes, leaving only the actuators on the exoskeleton and all the other components are installed elsewhere (other components are not even mentioned in some cases).

In addition, there are cases that they use a master-slave system to reduce the number of necessary components. For a master-slave system (i.e. Delft Cylinder Hand [36]), no pump, accumulator or reservoir are needed. Actuating a 'master' cylinder, in a close circuit, multiple 'slave' actuators can be controlled just with the use of valves. That information is very important to have in mind when optimizing the space that a hydraulic or pneumatic system needs to function properly.

Also, it is observed that McKibben soft actuators need less pressure to function, and according to Tiwari et al. [61] they have much higher force to weight ratio. Smart soft actuation systems have been analyzed [34-35, 39, 62-63] demonstrating that artificial muscles (even if they have the easiest construction procedure) are not the only soft actuation method that exist. On

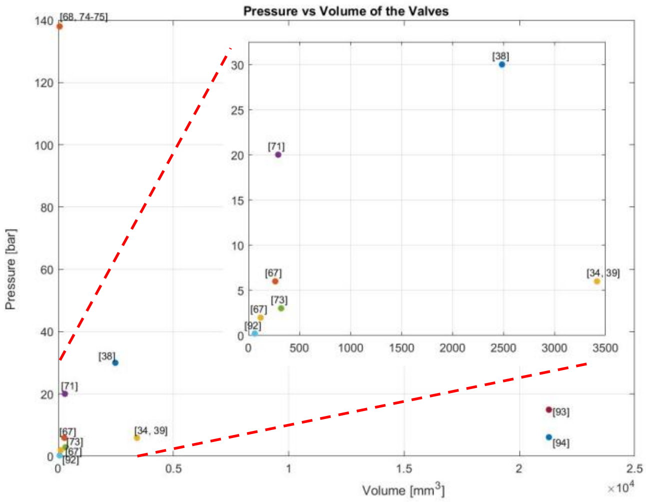

Fig. 26: Comparison of the valves of Table IV. Graphic representation of the pressure vs the volume of the valves. Inlet: Same graph focused on the left down corner.

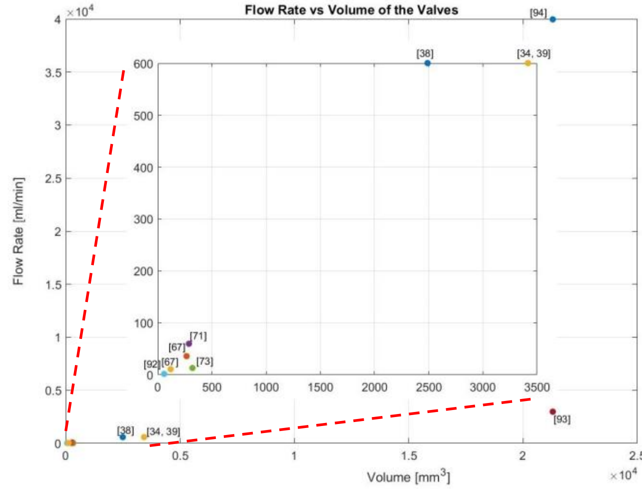

Fig. 27: Comparison of the valves of Table IV. Graphic representation of the flow rate vs the volume of the valves. Inlet: Same graph focused on the left down corner.

the other hand, a lot of knowledge exist on hard actuators (pistons and cylinders), and that makes the design, simulation and fabrication of such an actuator much easier. There are even studies that present a step-by-step guidance to calculate the right dimensions for a cylinder [64-65]. In contrast to Tiwari et al. [61], Plettenburg [66] demonstrated in 2005 that pneumatic artificial muscles have higher energy to weight ratio, but only compared with commercially available cylinders. Comparing an artificial muscle with commercially available as well as with a custom made cylinder, he proves that the commercially available cylinders are over-dimensioned with their energy to mass ratio to be smaller than the artificial muscle's ratio, while the artificial muscle compare to the custom made cylinder have 30 times smaller energy to mass ratio (stroke of 10 mm). This proves that custom made cylinders can indeed be more beneficial than the artificial muscles. Nevertheless, both hard and soft actuators have been developed, small enough to fit in a finger, between two joints (e.g. hard actuators: [36, 67], soft actuators: [35, 39, 68]), providing the required force for the actuation of an exoskeleton device.

Microfluidics on the other hand, seems that are not the best choice for a hand exoskeleton. The biggest problem is that they cannot work with high flow rates and as it was mentioned earlier, this will result to a slow motion of the movement. Li et al. [69-70] though, they manage to reach flow rates higher than 1000 ml/min by using an array of microfluidic valves. Their trick was to use multiple valves in parallel connection, resulting the addition of flow rate of each valve. Also, Roberts et al. [71-73] was investigating a way to amplify the displacement of a piezoelectric material used in a microfluidic valve, such that the resulting stroke of the valve's membrane will be large enough to allow higher flow rates.

There are a lot of different components available that someone can choose to develop a hydraulic or pneumatic hand exoskeleton. It is already proven that miniaturization is not a limiting factor for such a device. Sealing for both valves and actuators, is the most common problem in miniaturized components (causing leakages), and it is amplified by using higher pressures. Even so, a lot of hydraulic and pneumatic devices have been developed so far, with some of them having uniquely designed components that are covering all the special requirements needed [34-36, 39, 63, 68].

Even if hydraulics or pneumatics are not commonly used (compare to i.e. electric motors), it is possible to be used for the development of an exoskeleton device. Those systems can be very beneficial and with the correct choice of components, designing such a system can become much easier than an electronically actuated one (no additional mechanisms or gearing are needed).

Piezoelectrically and electromagnetically actuated valves that can work with the desirable (for a hand exoskeleton device) pressure and flow rate have already been developed. In addition microfluidic valves, even if they cannot work with high flow rates, have been used in smart configuration to allow flow rates more than 1000 ml/min (an array of more than 80 microfluidic non-return valves in parallel connection has been developed but the same principle could be used for other valves as well), which is more than enough for an exoskeleton. Fig. 26 and 27 compares the 2-way and 3-way hydraulic valves that have been used or developed in some studies. Only ten are compared because of the lack of information (see Table IV). Nevertheless, it can be observed that most of the valves work with pressures less than 30 bars, flow rate less than 100 ml/min and have a volume of less than 3500 mm^3. Using an actuator that could work with that pressure and flow rate can result to power of 5000 W (flow rate * pressure). Assuming an actuator volume of 3927 mm^3 (a diameter of 10 mm and length of 50 mm; those dimensions are assumed and correspond to the data that have been gathered as well as the maximum allowable volume calculated using equation 2 – Appendix I), the power to volume ratio was calculated to be 1272 × 106 Wm^{-3}. That is much higher than the ratio needed (calculated in Appendix I, equation 4 to be 2.73 × 106 Wm^3), proving that hydraulic valves small enough to fit on a hand exoskeleton, and also robust enough to

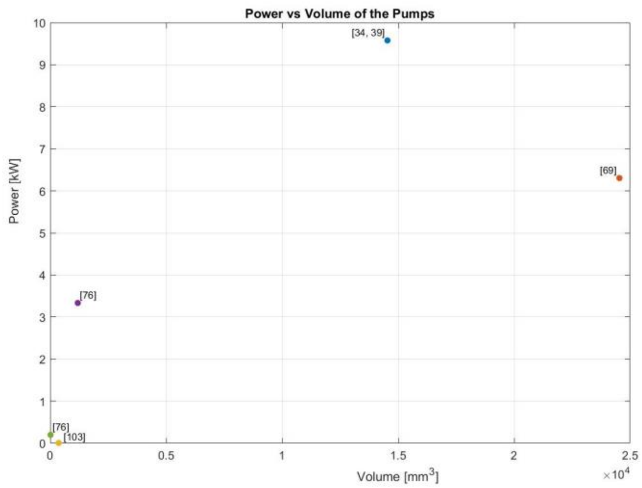

Fig. 28: Comparison of the pumps of Table V. Graphic representation of the power vs the volume of the pumps.

handle high pressures and flow rates, do exist and could be (or are already been) used. It is important to mention that valves that have higher volume than 0.5 × 104 mm^3, according to the requirements, cannot be used on a hand exoskeleton device. In addition, a valve with extremely high pressure and small volume can be observed (Love et al. [68, 74-75]). For that specific valve, no flow rate has been given and that is why it has been excluded from fig. 27. If the flow rate of such a valve is also high enough (see requirements – Section III), it could be the ideal valve to use on an exoskeleton or even a prosthetic device.

Regarding the pressurization of the fluid, miniaturized hydraulic pumps that can fit in the metacarpus of a hand prosthesis (equal or less than 25 mm on diameter and 50 mm length) have been presented, as well as master slave systems with the master cylinder to be actuated either manually (passive system) or with a motor. Studies that use hydraulic systems with a pump, also present miniaturized fluid reservoir that can fit with the pump and the valves in the metacarpus of the prosthetic device. Fig. 28 compares the power versus the volume of some hydraulic pumps that have been analyzed previously. In this comparison, only five pumps are included due to lack of information. It can be observed that three of them are small enough to fit on a hand exoskeleton device. The problem is that volume is not the only criterion, and it seems that two of them have a very low power (the power of the pumps has been calculated as the product of the pressure and the flow rate that the pump is able to provide). In just one case (Weisener et al. [76]), the power is high and also has a low volume (less than 0.5 × 104 mm^3).

Also, both hard and soft actuators that can produce enough force (or torque) and at the same time are small enough for a hand exoskeleton device exist and have been tested on prosthetics. In this case, no plot is represented due to lack of information (mostly flow rates; almost none of the studies gave a working flow rate of the hydraulic actuators used and that is why this information is also excluded from Table VI, but also in most of the cases not all of the dimensions are provided).

Even though miniaturized pumps as well as reservoirs already exist, the use of a master-slave system can be more beneficial. The lack of the weight and the volume of the pump, the accumulator and the reservoir, that a standard hydraulic device uses, can become an improvement on a similar device that uses a master-slave system instead. In addition, it is proven that smart joint actuation systems (that can save space and conclude to a more compact and cosmetically pleasing device) can be designed with the use of soft hydraulic or pneumatic actuators. Hard actuators on the other hand, having the standard cylindrical shape, are difficult (but not impossible) to be used in a smart design of a joint.

APPENDIX IV: EXPERIMENTAL DATA

The data gathered from the experiments are analytically represented in Table VII. For each design, the force was measured varying two factors: the angle and the pressure. The maximum pressure that was measured for each design was the "failure" pressure; meaning that the part failed at that specific pressure. The maximum ROM can also be obtained from the data. Using different pressures, different ROM can be succeeded, and that can be seen in Table VII. It is important to keep in mind that those data were measured to compare the different actuator designs. So, the final ROM cannot be obtained since two things have yet to be decided: a) the final design and b) the working pressure.

TABLE IV
QUANTITATIVE COMPARISON OF THE DIFFERENT VALVES

Reference	Type	Actuation method	Working fluid	Pmax (tested) [bar]	Qmax (tested) [ml/min]	Dimensions [mm]
Broome et al. [38]	Non-return valve	-	Vegetable oil	30	600	N.M.*
Broome et al. [38]	3-way valve	N.M.	Vegetable oil	30	600	12 Φ × 22
Broome et al. [36]	Relief valve	-	Vegetable oil	N.M.	N.M.	N.M.
Love et al. [68, 74-75]	2-way	SMA or magnetically	Liquid	138	N.M.	< 3 Φ × < 10 or < 2 Φ × < 16
Rodriguez [77]	Control valve	Electric motor	CO_2	N.M.	N.M.	N.M.
Rodriguez [77]	Relief valve	-	CO_2	N.M.	N.M.	N.M.
Bouzit et al. [40]	Commercially available valve with 8 internal microvalves (Matrix)	N.M.	Gas	N.M.	N.M.	N.M.
DiCicco et al. [78]	Commercially available valve (Herion 4088X)	N.M.	Gas	8.3	N.M.	N.M.
Allington et al. [79]	Commercially available solenoid on/off valve (Matrix 821)	N.M.	Air	6	950	N.M.
Pylatiuk et al. [80]	3/2-way commercially available picosol valve (FAS)	N.M.	Gas or liquid	N.M.	N.M.	< 30 × < 12 × < 7
Plygerinos et al. [23-24]	Commercially available solenoid valve (MC202-VB30)	N.M.	Water	4	N.M.	N.M.
Schylz et al. [35]	Microvalve	N.M.	Liquid	0.5	N.M.	N.M.
Schulz et al. and Kargov et al. [34, 39]	2-way normally closed valve	Electrically actuated	Non-toxic biocompatible oil	6	600	23.47 × 11.2 × 13
Kline et al. [81]	Commercially available relief valve	-	Gas	Open pressure**: 0.42	N.M.	N.M.
Kline et al. [81]	Commecially available control valve	Servo actuated	Gas	0.35	N.M.	N.M.
Xing et al. [82]	Control valve	Electrically actuated	Gas	4	N.M.	N.M.
Wu et al. [83]	Commercially available control valve (ITV 1030-211BS)	Electromagnetically actuated	Gas	5	N.M.	N.M.
Wu et al. [83]	Commercially available pressure regulating valve (AW20-02BCG)	N.M.	Gas	8.5	N.M.	N.M.
Tadano et al. [41]	Commercially available spool valve (FESTO)	Servo actuated	Gas	6	N.M.	N.M.
Kiminori et al. [42]	Air regulator valve	Electrically actuated	Gas	3.5	N.M.	N.M.
Chakraborty et al. [84]	One way normally closed microfluidic valve	Piezoelectrically actuated	Air	2.4	900	16 × 16
Roberts et al. [71]	Hydraulic amplification microfluidic control valve	Piezoelectrically actuated	Liquid	20	60	12 × 12 × 2
Roberts et al. [73]	Hydraulic amplification microfluidic control valve	Piezoelectrically actuated	Liquid	> 3	> 12.6	8 × 8 × 5
Rogge et al. [85]	Hydraulic amplification normally closed microfluidic valve	Piezoelectrically actuated	Nitrogen (N_2) or water	N_2: 2 or Water: 1	N_2: 700 ml/min	13 × 13 × 3

* Not mentioned.
** Open pressure refers to the minimum pressure needed to open the relief or in other words the maximum operating pressure.

TABLE IV
QUANTITATIVE COMPARISON OF THE DIFFERENT VALVES (CONTINUES)

Reference	Type	Actuation method	Working fluid	Pmax (tested) [bar]	Qmax (tested) [ml/min]	Dimensions [mm]
Yang and Lin [86]	Non-return microfluidic valve	-	DI water***	1.7	4	N.M.
Yang and Lin [86]	Non-return microfluidic valve	-	DI water	0.375	4	N.M.
Yang and Lin [86]	Non-return microfluidic valve	-	DI water	2	1.2	N.M.
Li et al. [69]	Non-return microfluidic valves array	-	DI water	100	1080 @ 3.5 bar	12 Φ
Li and Chen [70]	Non-return microfluidic valves array	Opening pressure of 0.3 bar	DI water	100	1140 @ 6.7 bar	12 Φ
Klasson [87]	Pressure regulator valve	N.M.	Gas	N.M.	N.M.	30 Φ × 21
Pistecky & Cool and Pistecky [88-89]	Normally closed valve	Electrically actuated	Gas	N.M.	N.M.	3 Φ × 20
Hekman & Plettenburg [90, 43]	Switch valve	Mechanically operated	Gas	12	N.M.	3 Φ × 4.3
Plettenburg [43]	Relay spool type valve	Pneumatic pulse of ΔP = 4 bar	Gas	12	1250	3.5 Φ × 8.15
Esashi [91]	Normally open valve	Piezoelectrically actuated	Gas	N.M.	N.M.	3 × 14 × 9
Esashi [91]	Normally closed valve	Piezoelectrically actuated	Gas	0.73	50	N.M.
Gongora-Rudio [92]	Normally closed valve	Electromagnetically actuated	Liquid	0.2	1.5	12 × 12 × 0.4
Yoo and Wereley [93]	Magnetorheological valve	Electromagnetically actuated	Liquid	15	3000	25.4 Φ × 42
Tu et al. [94]	3-way rotary on/off valve	Electric motor	Liquid	6.2	40000	25.4 Φ × 98
Peirs et al. [67]	2-way normally open valve	Piezoelectrically actuated	Water	6	36	15 × 3.5 × 5
Peirs et al. [67]	2-way normally open valve	Electromagnetically actuated	Water	2	10.8	< 3.5 Φ × 12
Bryant et al. [95]	Commercially available 4/2 directional valve	Servo actuated	50-50 water and ethylene glycol mixture	6.2	N.M.	N.M.

*** Deionized water

TABLE V
QUANTITATIVE COMPARISON OF THE DIFFERENT PUMPS

Reference	Pumping Technique	Actuation	Working Frequency [Hz]	Working fluid	Pmax (tested) [bar]	Qmax (tested) [ml/min]	Dimensions [mm]	Power Consumption [W]
Broome et al. [38]	Rotary	Electric motor	N.M.	Vegetable oil	30	600	N.M.	N.M.
Pylatiuk et al.[80]	Rotary/Two-way operation	Electric motor	N.M.	Gas or liquid	N.M.	N.M.	21 $\Phi \times 42$	N.M.
Polygerinos et al. [23-24]	Vibrating diaphragm	N.M.	N.M.	Water	4	N.M.	N.M.	9.6
Schulz et al. and Kargov et al. [34, 39]	Rotary/External gear	Electric motor	N.M.	Non-toxic biocompatible oil	9.2	625	21 $\Phi \times 42$	18.9
Li et al. [69]	Vibrating diaphragm	Piezoelectric	10000	DI water	24	1080 @ 3.5 bar	25 $\Phi \times 50$	N.M.
Kamper et al. [96]	Vibrating diaphragm	Piezoelectric	70	Water	2	0.45	N.M. (microfluidic)	N.M.
Park et al. [97]	Vibrating diaphragm	Piezoelectric	850	Water	2.5	6	N.M. (microfluidic)	N.M.
Park et al. [98]	Vibrating diaphragm	Piezoelectric	2200	Water	3.2	6.6	N.M. (microfluidic)	N.M.
Zeng et al. [99]	Electroosmotic	-	-	Liquid	36.3	0.017	N.M. (microfluidic)	N.M.
Paul et al. [100]	Electrokinetic	-	-	Liquid	10	0.03×10^{-3}	N.M. (microfluidic)	N.M.
Paul et al. [101]	Electroosmotic	-	-	Liquid	345	N.M.	N.M. (microfluidic)	N.M.
Li et al. [102]	Vibrating diaphragm	Piezoelectric	4.5	Liquid	8.5	3	N.M. (microfluidic)	N.M.
Doll et al. [103]	Vibrating diaphragm	Piezoelectric (4-membrane)	25.3	Liquid	0.6	4.2	$30 \times 12 \times 1$	N.M.
Doll et al. [103]	Vibrating diaphragm	Piezoelectric (3-membrane)	35	Liquid	0.75	4	N.M. (microfluidic)	N.M.
Weisener et al. [76]	Rotary	Electric motor	N.M.	Liquid	50	200 @ 10 bar	10 $\Phi \times 15$	N.M.
Weisener et al. [76]	Rotary	Electric motor	N.M.	Liquid	15	8	2.5 $\Phi \times 4$	N.M.
Kim et al. [104]	Vacuum	N.M.	1	Gas	0.5	N.M.	$18 \times 25 \times 5.5$	3.6
Son et al. [105]	Vacuum	N.M.	1	Gas	0.3	11.36	26.5 $\Phi \times 13.5$	0.7
Al-Halhouli et al. [106]	Electromechanical/piston-acting magnet	Electromagnet	N.M.	Water	0.004	6.1	18 Φ	N.M.
Bryant et al. [95]	Rotary	Electric motor	N.M.	50-50 water and ethylene glycol mixture	10	800 @ 8 bar	N.M.	N.M.

TABLE VI
QUANTITATIVE COMPARISON OF THE DIFFERENT ACTUATORS

Reference	Actuator type	Working fluid	Stroke [mm]	Pmax (tested) [bar]	Force [N]	Dimensions [mm]
Heather and Smith [37]	Hydraulic cylinder	Water	25.4	10	330	12.7 Φ
Broom et al. [38]	Double acting hydraulic cylinder	Vegetable oil	N.M.	30	1000	N.M.
Smit et al. [36]	Hydraulic cylinder	Liquid	N.M.	60	30	Smallest: 7 Φ Larger: 10 Φ
Love et al. [68]	Flexing hydraulic actuator	Liquid	7.6	138	10	2.3 Φ
Love et al. [68]	Flexing hydraulic actuator	Liquid	35.4	138	87	9.6 Φ
Bouzit et al. [40]	Pneumatic cylinder	Gas	45%	N.M.	>50	Length: 40-60
Lee and Ryu [33]	Hydraulic artificial muscle	Water	3.46	5.5	4	2 Φ
Pylatiuk et al. [80]	Flexible fluidic actuator	Gas or liquid	N.M.	N.M.	Torque: 3Nm	20 Φ
Schylz et al. [35]	Miniaturized flexible fluidic bladders	Liquid	N.M.	0.5	3	N.M.
Schulz et al. and Kargov et al. [34, 39]	Flexible fluidic actuator	Non-toxic biocompatible oil	N.M.	6	Torque: 0.69Nm	12 $\Phi \times 16$
Noritsugu et al. [107]	Curved rubber muscles	Gas	N.M.	5	23	16 Φ
Sasaki [108]	McKibben artificial muscle	Gas	N.M.	5	Torque: 300Nmm	28 $\Phi \times 180$
Kline et al. [81]	Single chamber bladder	Gas	N.M.	0.35	Torque: <1Nm	-
Xing et al. [82]	McKibben artificial muscle	Air	25%	4	130	14 $\Phi \times 210$ 14 $\Phi \times 240$
Tadano et al. [41]	Artificial rubber muscle	Gas	20%	6	20	Inner Φ 5
Kiminori et al. [42]	Soft actuators	Gas	N.M.	3.5	3.5	N.M.
Garcia-Bonito et al. [109]	Piezo-electric piston type	Ethylene glycol	7×10^{-9} m/V (per unit voltage)	N.M.	0.015 N/V (per unit voltage)	44.44 $\Phi \times 38.1$
Menon and Lira [63]	Flexible joint "Smart Stick" mechanism	Liquid	N.M.	12	N.M.	1 Φ
Peirs et al. [67]	Piston type	Liquid	10	10	7	Inner Φ 3
Bryant et al. [95]	McKibben hydraulic artificial muscle	50-50 water and ethylene glycol mixture	N.M.	6.2	100	6.25 $\Phi \times 177.8$

TABLE VII
EXPERIMENTAL DATA

Pressure [bar]	**ROM [Deg]**																				
	0	**5**	**10**	**15**	**20**	**25**	**30**	**35**	**40**	**45**	**50**	**55**	**60**	**65**	**70**	**75**	**80**	**85**	**90**	**95**	**100**
1st Design																					
0.5	0.035	0.03	0.023	0.012	0	0	0	0	0	0	0	0	0	0							
1	0.047	0.04	0.035	0.023	0.011	0	0	0	0	0	0	0	0	0							
1.2	0.058	0.047	0.047	0.035	0.035	0.023	0.023	0.012	0	0	0	0	0	0							
1.4	0.082	0.086	0.082	0.058	0.047	0.028	0.028	0.023	0.012	0	0	0	0	0							
1.6	0.1	0.094	0.105	0.093	0.08	0.047	0.035	0.035	0.047	0.035	0.035	0.023	0.023	0.011							
1.8	0.21	0.234	0.21	0.198	0.187	0.187	0.175	0.14	0.105	0.093	-	-	-	-							
2nd Design																					
0.5	0.023	0.047	0.047	0.047	0.047	0.035	0.035	0.035	0.012	0	0	0	0	0	0	0	0	0	0		
1	0.058	0.047	0.047	0.047	0.035	0.035	0.035	0.035	0.035	0.023	0.023	0.023	0.012	0.012	0	0	0	0	0		
1.2	0.128	0.105	0.105	0.093	0.093	0.093	0.088	0.07	0.07	0.07	0.058	0.047	0.047	0.035	0.04	0.023	0.012	0.012	0		
1.4	0.175	0.129	0.117	0.117	0.105	0.105	0.105	0.093	0.082	0.07	0.058	0.058	0.047	0.035	0.04	0.035	0.023	0.012	0.012		
3rd Design																					
0.5	0.035	0.035	0.023	0.023	0.023	0.012	0.012	0.012	0	0	0	0	0	0	0	0	0	0	0	0	0
1	0.07	0.07	0.047	0.047	0.035	0.035	0.035	0.023	0.023	0.012	0	0	0	0	0	0	0	0	0	0	0
1.2	0.128	0.105	0.093	0.093	0.082	0.082	0.082	0.07	0.058	0.058	0.047	0.035	0.035	0.023	0.012	0.012	0	0	0	0	0
1.4	0.175	0.175	0.175	0.164	0.164	0.164	0.164	0.152	0.14	0.117	0.105	0.093	0.082	0.07	0.058	0.047	0.035	0.023	0.023	0.012	0.012
4th Design																					
0.5	0.035	0.023	0.012	0.012	0	0	0	0	0	0	0	0	0	0	0	0					
1	0.058	0.047	0.023	0.023	0.012	0	0	0	0	0	0	0	0	0	0	0					
1.2	0.105	0.093	0.07	0.058	0.047	0.035	0.023	0.012	0	0	0	0	0	0	0	0					
1.4	0.14	0.128	0.105	0.082	0.07	0.07	0.047	0.035	0.023	0.012	0	0	0	0	0	0					
1.6	0.187	0.164	0.14	0.129	0.117	0.105	0.093	0.07	0.058	0.047	0.035	0.023	0	0	0	0					
1.8	0.222	0.199	0.187	0.175	0.164	0.152	0.14	0.117	0.105	0.093	0.07	0.058	0.035	0.023	0.023	0.012					
2	0.316	0.292	0.292	0.28	0.269	0.259	0.245	-	-	-	-	-	-	-	-	-					
5th Design																					
0.5	0.0234	0.0116	0	0	0	0	0	0	0	0	0	0									
1	0.035	0.0116	0	0	0	0	0	0	0	0	0	0									

1.2	0.07	0.035	0.012	0	0	0	0	0	0	0	0	0						
1.4	0.093	0.07	0.035	0.023	0	0	0	0	0	0	0	0						
1.6	0.127	0.093	0.07	0.047	0.035	0.012	0	0	0	0	0	0						
1.8	0.164	0.117	0.105	0.089	0.07	0.047	0.023	0	0	0	0	0						
2	0.199	0.152	0.129	0.105	0.093	0.07	0.047	0.023	0	0	0	0						
2.2	0.234	0.199	0.175	0.14	0.129	0.117	0.093	0.07	0.035	0.023	0	0						
2.4	0.269	0.222	0.21	0.187	0.175	0.164	0.128	0.112	0.082	0.058	0.035	0.012						
6th Design																		
0.5	0.0234	0.0116	0	0	0	0	0	0										
1	0.035	0.0116	0	0	0	0	0	0										
1.2	0.07	0.035	0.0116	0	0	0	0	0										
1.4	0.1051	0.07	0.035	0.0234	0.0116	0	0	0										
1.6	0.1401	0.1051	0.07	0.0467	0.035	0.0116	0	0										
1.8	0.1753	0.1285	0.1051	0.0818	0.07	0.0467	0.0234	0										
2	0.2103	0.1752	0.1402	0.1285	0.1051	0.0817	0.0584	0.035										
Pressurized Water																		
0.85	0.058	0.047	0.035	0.035	0.035	0.023	0	0	0	0	0	0	0	0	0	0	0	0
1.4	0.093	0.082	0.082	0.07	0.058	0.058	0.047	0.047	0.035	0.023	0.023	0	0	0	0	0	0	0
1.8	0.152	0.129	0.129	0.117	0.117	0.105	0.093	0.082	0.07	0.058	0.047	0.035	0.023	0.023	0	0	0	0
2.2	0.257	0.234	0.234	0.199	0.187	0.164	0.14	0.129	0.105	0.082	0.07	0.058	0.047	0.035	0.035	0.023	0.023	0.023
2.6	0.341	0.316	0.29	0.269	0.245	0.199	0.187	0.164	0.152	0.105	0.093	0.07	0.059	0.047	0.035	0.023	0.023	0.023
3	0.397	0.397	0.362	0.304	0.292	0.245	0.21	0.187	0.152	0.129	0.105	-	-	-	-	-	-	-